Synthesis of geared five-bar linkages through continuation methods

by

Gloria K. Starns

A Thesis Submitted to the
Graduate Faculty in Partial Fulfillment of the
Requirements for the Degree of
MASTER OF SCIENCE

Major: Mechanical Engineering

Signatures have been redacted for privacy

Signatures have been redacted for privacy

Iowa State University
Ames, Iowa
1990

TABLE OF CONTENTS

LIST OF TABLES

LIST OF FIGURES

ABSTRACT

This document demonstrates the synthesis of geared five-bar path generating mechanisms using continuation methods. The gear ratio can be varied resulting in a solution set of geared five-bars passing through seven prescribed positions. Additionally it will be demonstrated that the gearing configuration may be altered and that continuation methods will produce a solution set of geared five-bars with an alternate gear configuration generating a prescribed path.

This development differs from past approaches in that convergence of the synthesis equations to a solution is not dependent on the choice of initial values and, furthermore, all solutions to the five precision point, four-bar synthesis problem are found. The method can be employed by a designer to select a geared-five bar path generator with a wide range of possible gear ratios.

ACKNOWLEDGEMENTS

My gratitude and respect to Mr. Thiagaraj Subbian who expertly and patiently introduced me to continuation methods and their implementation.

CHAPTER 1. INTRODUCTION

Historically, geared five-bar path generation mechanisms have been designed graphically or through synthesis equations requiring iterative techniques. A relatively new numerical method that solves systems of polynomial equations, the continuation method, may be implemented to solve polynomial systems occurring in kinematic synthesis. The continuation method of synthesis provides a twofold advantage over past methods. First, the method does not require "close" initial guesses, and secondly, all solutions to the *first* of three continuation methods implemented are generated. The continuation method tracks the variables from a start system to a system for which solutions are sought through an independent parameter. The system for which solutions are sought is referred to in the majority of the literature as the "target" system.

Freudenstein and Roth (1963) in their development of a geared five-bar synthesis method reduced loop closure equations to one non-linear equation per precision point. The authors first eliminated various nonessential parameters and then implemented a "bootstrap" method that employed techniques similar to continuation methods.

More recently continuation methods have been used to synthesize four-bar path generation mechanisms. Subbian and Flugrad (1989) presented methods resulting in all designs passing through five precision points. Morgan and Wampler (1989)

also solved the five precision point, four-bar synthesis problem through polynomial continuation. Likewise, Tsai and Lu (1989) employed a homotopy method that generated four-bar linkages passing though nine precision points. Wampler, Morgan and Sommese (1990) demonstrated the solution to the kinematic synthesis of four-bar mechanisms passing through nine precision points using polynomial continuation. They identified 4326 distinct solutions, inclusive of Robert's cognates.

The treatment of geared five-bar mechanisms has been addressed by Sandor and Kaufman et al. (1969) and by Freudenstein and Roth (1963). Recently Dhingra and Mani (1988) presented closed form solutions for the synthesis of geared mechanisms generating a specified function. Subbian and Flugrad (1990) implemented continuation methods to accomplish motion generation with prescribed timing resulting in an eight-bar linkage passing through six precision points. The same authors, in the same paper, also demonstrated synthesis of a geared five-bar passing through seven precision points employing triad (a triplet combination of vectors) synthesis through continuation.

The synthesis of a geared five-bar mechanism with a varying gear ratio may be accomplished purely through continuation techniques beginning with solutions generated by continuation methods in the synthesis of a four-bar mechanism. Additional precision points may be added to the four-bar mechanism's path by modifying and adding additional continuation equations referred to as homotopy functions. Following synthesis of a four-bar linkage passing through a desired number of precision points, one of three five-bar cognates predicted by Robert's theorem may be selected as the start system for the third continuation algorithm. The third continuation procedure provides the designer a solution set of geared linkages that will satisfy the

path specifications. This solution set may be plotted against a varying gear ratio.

Finally, the synthesis of a geared five-bar with gears centered about moving pivot points is developed using continuation. The gear ratio is varied in this synthesis method as well, again resulting in a solution set of geared linkages.

CHAPTER 2. FOUR-BAR - SEVEN PRECISION POINTS

Alexander Morgan (1987) notes in *Solving Polynomial Systems Using Continuation For Engineering and Scientific Problems* that continuation is a "global and exhaustive" numerical method for solving small polynomial systems. Continuation, Morgan points out, finds all solutions to the system of equations and does not require prior knowledge of the system solutions.

Essentially, continuation consists of two systems; the first is a simple system that provides values at the start of a continuation path; the second system is the target system or the system for which solutions are desired. Tracking and following a path from the start system to the target system identifies solutions to the target system. Morgan also cites Bezout's theorem which enables the designer to identify the number of solutions that exist.

The applications of continuation methods to kinematic synthesis are particularly useful as many equations of synthesis lend themselves well to expression in polynomial form. The objective of the following presentation is to demonstrate the application of continuation methods to first design a single geared five-bar mechanism passing through seven precision points and, secondly, to demonstrate a continuation method which enables a designer to synthesize a set of five-bar mechanisms with varying gear ratios.

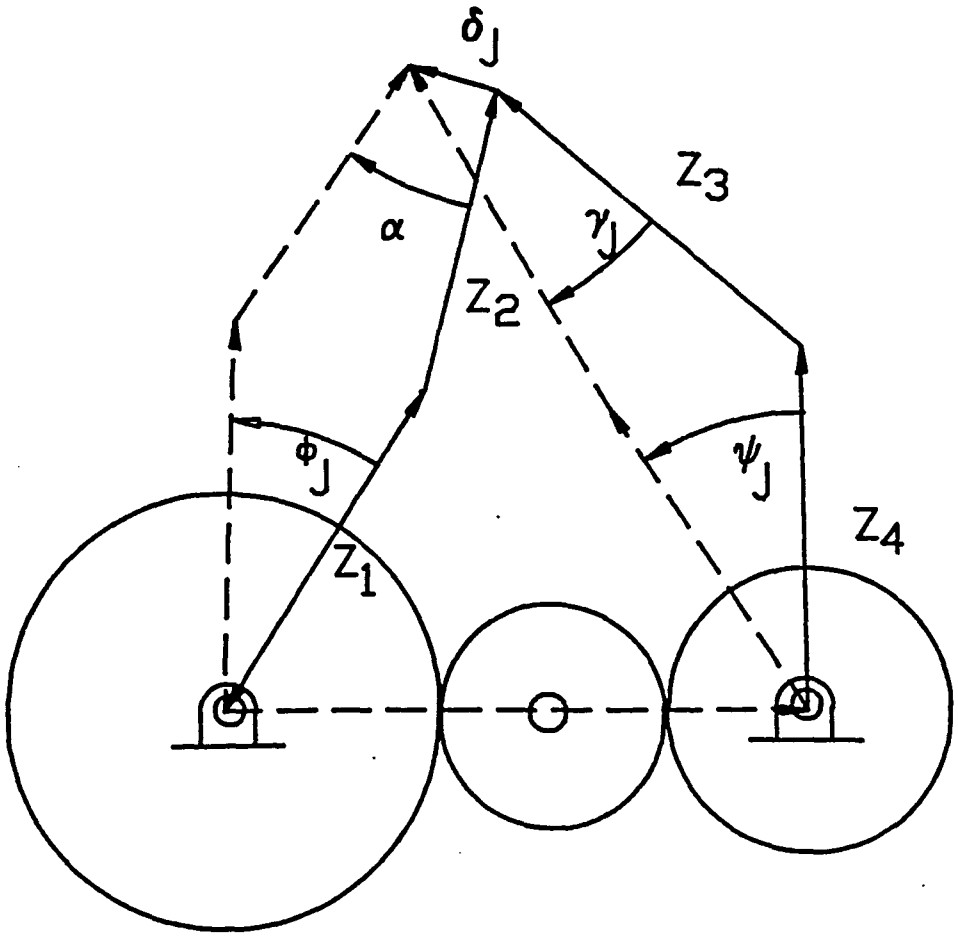

Figure 2.1: Five-bar mechanism in the jth position

Figure 2.1 schematically depicts the displacement of a five-bar mechanism from its initial position to a subsequent position, j. Loop closure equations for each combination of vector pairs, or dyads, result in the following as established by Freudenstein and Roth (1963):

$$\begin{aligned} DYAD\ 1: \mathbf{Z_1}e^{i\phi_j} + \mathbf{Z_2}e^{i\alpha_j} &= \delta_j + \mathbf{Z_1} + \mathbf{Z_2} \\ DYAD\ 2: \mathbf{Z_4}e^{i\psi_j} + \mathbf{Z_3}e^{i\gamma_j} &= \delta_j + \mathbf{Z_4} + \mathbf{Z_3} \end{aligned} \tag{2.1}$$

Rearrangement of Eq.(2.1) produces:

$$\begin{aligned} \mathbf{Z_1}(e^{i\phi_j} - 1) + \mathbf{Z_2}(e^{i\alpha_j} - 1) &= \delta_j \\ \mathbf{Z_4}(e^{i\psi_j} - 1) + \mathbf{Z_3}(e^{i\gamma_j} - 1) &= \delta_j \end{aligned} \tag{2.2}$$

Parameters α_j and γ_j may be eliminated since they are not of interest here. To accomplish this, real and imaginary components are first separated:

$$\delta_{xj} = Z_{1x}cos\phi_j - Z_{1x} - Z_{1y}sin\phi_j + Z_{2x}cos\alpha_j - Z_{2x} - Z_{2y}sin\alpha_j \tag{2.3}$$

$$\delta_{yj} = Z_{1x}sin\phi_j + Z_{1y}cos\phi_j - Z_{1y} + Z_{2x}sin\alpha_j + Z_{2y}cos\alpha_j - Z_{2y} \tag{2.4}$$

$$\delta_{xj} = Z_{4x}cos\psi_j - Z_{4x} - Z_{4y}sin\psi_j + Z_{3x}cos\gamma_j - Z_{3x} - Z_{3y}sin\gamma_j \tag{2.5}$$

$$\delta_{yj} = Z_{4x}sin\psi_j + Z_{4y}cos\psi_j - Z_{4y} + Z_{3x}sin\gamma_j + Z_{3y}cos\gamma_j - Z_{3y} \tag{2.6}$$

Expressions for $sin\alpha_j$ and $cos\alpha_j$ are developed as follows from Eqs. (2.3-2.6). First, Eq.(2.3) is multiplied by $-Z_{2y}$ then Eq.(2.4) is multiplied by Z_{2x}. The results of each multiplication are added to produce:

$$\begin{aligned} sin\alpha_j = {} & (-Z_{2y}\delta_{xj} + Z_{2x}\delta_{yj} + Z_{2y}Z_{1x}cos\phi_j - Z_{1x}Z_{2x}sin\phi_j \\ & - Z_{2y}Z_{1x} - Z_{1y}Z_{2x}cos\phi_j - Z_{2y}Z_{1y}sin\phi_j + Z_{1y}Z_{2x}) \\ & / \ (Z_{2x}^2 + Z_{2y}^2) \end{aligned} \tag{2.7}$$

Likewise Eq.(2.3) is multiplied by Z_{2x} and added to the product of Eq.(2.4) and Z_{2y}. This results in an expression for $cos\alpha_j$:

$$\begin{aligned} cos\alpha_j &= (Z_{2x}\delta_{xj} + Z_{2y}\delta_{yj} + Z_{2x}^2 + Z_{2y}^2 - Z_{1x}Z_{2x}cos\phi_j - Z_{1y}Z_{2y}cos\phi_j \\ &- Z_{1x}Z_{2y}sin\phi_j + Z_{1y}Z_{2x}sin\phi_j + Z_{2x}Z_{1x} + Z_{2y}Z_{1y}) \\ &/ (Z_{2x}^2 + Z_{2y}^2) \end{aligned} \tag{2.8}$$

Similar treatment of equations (2.5) and (2.6) results in expressions for $sin\gamma_j$ and $cos\gamma_j$.

$$\begin{aligned} sin\gamma_j &= (-Z_{3y}\delta_{xj} + Z_{3x}\delta_{yj} + Z_{4x}Z_{3y}cos\psi_j - Z_{4x}Z_{3x}sin\psi_j \\ &- Z_{3y}Z_{4x} - Z_{3x}Z_{4y}cos\psi_j - Z_{4y}Z_{3y}sin\psi_j + Z_{3x}Z_{4y}) \\ &/ (Z_{3y}^2 + Z_{3x}^2) \end{aligned} \tag{2.9}$$

$$\begin{aligned} cos\gamma_j &= (Z_{3x}\delta_{xj} + Z_{3y}\delta_{yj} + Z_{3x}^2 + Z_{3y}^2 - Z_{3x}Z_{4x}cos\psi_j - Z_{3y}Z_{4x}sin\psi_j \\ &+ Z_{3x}Z_{4x} - Z_{3y}Z_{4y}cos\psi_j + Z_{3x}Z_{4y}sin\psi_j Z_{3y}Z_{4y}) \\ &/ (Z_{3y}^2 + Z_{3x}^2) \end{aligned} \tag{2.10}$$

Substitution of Eqs. (2.7-2.10) into the trigonometric identities $sin^2\alpha_j + cos^2\alpha_j = 1$ and $sin^2\gamma_j + cos^2\gamma_j = 1$ yield the following:

$$\begin{aligned} 2A_{1j}s\phi_j + 2(1 - c\phi_j)B_{1j} + D_{1j} &= 0 \\ 2A_{2j}s\psi_j + 2(1 - c\psi_j)B_{2j} + D_{2j} &= 0 \end{aligned} \tag{2.11}$$

where:

$$\begin{aligned} A_{1j} &= Z_{1y}Z_{2x} - Z_{2y}Z_{1x} + Z_{1y}\delta_{xj} - Z_{1x}\delta_{yj} \\ B_{1j} &= Z_{1x}^2 + Z_{1y}^2 + Z_{1x}Z_{2x} + Z_{1y}Z_{2y} + Z_{1x}\delta_{xj} + Z_{1y}\delta_{yj} \end{aligned}$$

$$
\begin{aligned}
D_{1j} &= 2Z_{2y}\delta_{yj} + 2Z_{2x}\delta_{xj} + \delta_{xj}^2 + \delta_{yj}^2 \\
A_{2j} &= Z_{4y}Z_{3x} - Z_{3y}Z_{4x} + Z_{4y}\delta_{xj} - Z_{4x}\delta_{yj} \\
B_{2j} &= Z_{4x}^2 + Z_{4y}^2 + Z_{3y}Z_{4y} + Z_{3x}Z_{4x} + Z_{4x}\delta_{xj} + Z_{4y}\delta_{yj} \\
D_{2j} &= 2Z_{3x}\delta_{xj} + 2Z_{3y}\delta_{yj} + \delta_{xj}^2 + \delta_{yj}^2
\end{aligned} \tag{2.12}
$$

Figure 2.2 depicts a four-bar mechanism in two finitely separated positions. Loop closure equations yield expressions identical to those of Eq. (2.1). The four-bar's coupler link, with vectors $Z_2 - Z_3 - A$, rotates through a displacement γ_j, which is equal to α_j. Also, in the case of the four-bar, the constraint of a gearing relationship between input and output displacements is absent. Consequently, the best choice for parameters to be eliminated are ϕ_j and ψ_j, which represent rotations of links Z_1 and Z_4 respectively. Algebraic manipulation and trigonometric substitution similar to the previously detailed method, result in the following for the four-bar:

$$
\begin{aligned}
DYAD\ 1 : 2A_{1j}sin\gamma_j - 2B_{1j}cos\gamma_j &= -2B_{1j} - D_{1j} \\
DYAD\ 2 : 2A_{2j}sin\gamma_j - 2B_{1j}cos\gamma_j &= -2B_{2j} - D_{2j}
\end{aligned} \tag{2.13}
$$

Solving these expressions for $sin\gamma_j$ and $cos\gamma_j$ we find,

$$
\begin{aligned}
sin\gamma_j &= (B_{1j}D_{2j} - B_{2j}D_{1j})/2(A_{1j}B_{2j} - A_{2j}B_{1j}) \\
cos\gamma_j &= 1 + (A_{1j}D_{2j} - A_{2j}D_{1j})/2(A_{1j}B_{2j} - A_{2j}B_{1j}) \quad .
\end{aligned} \tag{2.14}
$$

Then invoking the trigonometric identity, $sin^2\gamma_j + cos^2\gamma_j = 1$, one may form the following expression,

$$
\begin{aligned}
F_j &= (B_{1j}D_{2j} - B_{2j}D_{1j})^2 \\
&+ 4(A_{1j}B_{2j} - A_{2j}B_{1j})(A_{1j}D_{2j} - A_{2j}D_{1j}) \\
&+ (A_{1j}D_{2j} - A_{2j}D_{1j})^2
\end{aligned} \tag{2.15}
$$

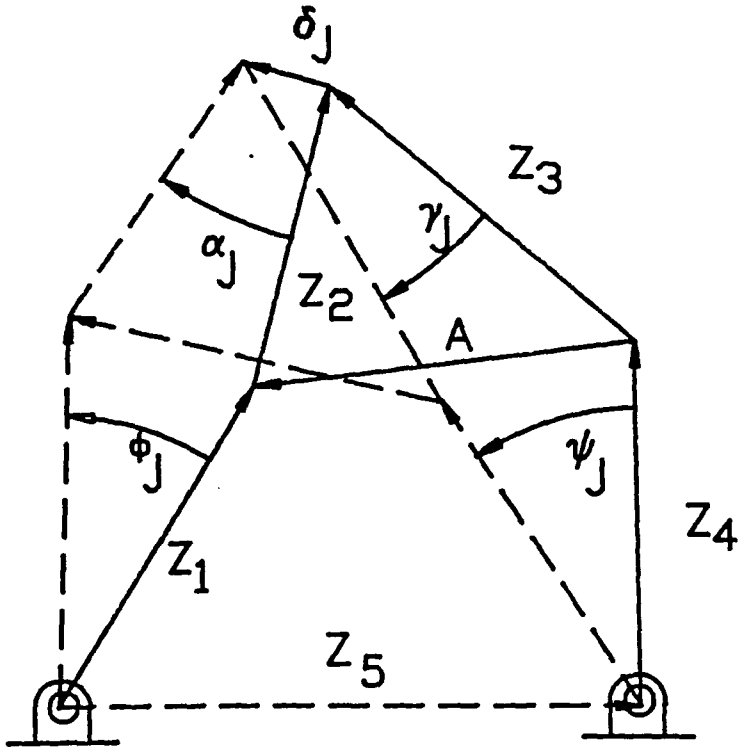

Figure 2.2: Four-bar mechanism in the jth position

Equation (2.15) was used as the target system in the homotopy function noted below by Subbian and Flugrad (1989) in their development of continuation methods for synthesis of four-bar mechanisms.

$$H(Z_j,t) = tF(Z_j) + (1-t)G(Z_j) \tag{2.16}$$

$G(Z_j)$ is the start system and t, the homotopy parameter, is the independent variable for integration of terms resulting in solutions to $F(Z_j)$.

The development by Subbian and Flugrad (1989) lends itself to further application in the synthesis of geared five-bar mechanisms. By modifying the start system, $G(Z_j)$, four-bar mechanisms passing through seven precision points can be generated by continuation. It should be noted that this particular continuation procedure is heurestic in nature. Also, the continuation method described below finds *some* of the solutions to the seven point four-bar synthesis problem whereas the preceding development found *all* solutions.

Tsai and Lu (1989) implemented a "cheaters homotopy" (Li, Sauer, and Yorke (1986)) function to synthesize four-bar linkages passing through nine precision points. However, the "cheaters homotopy" requires that random complex numbers be added to the start system to ensure the smoothness and accessibility properties of the homotopy.

Wampler, Morgan and Sommese (1982) suggested the following function as being sufficient for the requirements of an acceptable homotopy,

$$H(Z_j,t) = (1-t)e^{i\theta}G(Z_j) + tF(Z_j) \tag{2.17}$$

In the above expression, t is the homotopy parameter, $G(Z_j)$ is the start system and $F(Z_j)$ is the system for which solutions are sought. The parameter θ is a randomly

chosen constant incorporated in the function to prevent premature vanishing of the homotopy and it additionally provides "complexified" homotopy functions. For synthesis of the original four-bar with a coupler point passing through five precision points, the target system, $F(Z_j)$, derived by Subbian and Flugrad (1989) and modeled by Eq. (2.15) was used. For the second stage of the process, where two more precision points were added to the coupler path, the start system, $G(Z_j)$, for each of the five original precision points was made the same as the target system, $F(Z_j)$. For the two newly prescribed precision points the start system was not equal to the target system but instead contained precision points on the beginning mechanism's coupler curve. These precision points were those closest in magnitude, direction, and timing to the two newly designated points. Therefore, as the homotopy parameter, t, approached unity, the initial coupler curve containing five precision points "moved toward" the curve containing the original five plus the two new coupler points.

The seven point synthesis algorithm requires determination of the system's Jacobian matrix, augmented by the partial derivative of the homotopy function with respect to the homotopy parameter. In matrix form:

$$\begin{bmatrix} \frac{\partial H_1}{\partial Z_{1x}} & \frac{\partial H_1}{\partial Z_{1y}} & \frac{\partial H_1}{\partial Z_{2x}} & \frac{\partial H_1}{\partial Z_{2y}} & \frac{\partial H_1}{\partial Z_{4x}} & \frac{\partial H_1}{\partial Z_{4y}} & \frac{\partial H_1}{\partial t} \\ \frac{\partial H_2}{\partial Z_{1x}} & \frac{\partial H_2}{\partial Z_{1y}} & \frac{\partial H_2}{\partial Z_{2x}} & \frac{\partial H_2}{\partial Z_{2y}} & \frac{\partial H_2}{\partial Z_{4x}} & \frac{\partial H_2}{\partial Z_{4y}} & \frac{\partial H_2}{\partial t} \\ \frac{\partial H_3}{\partial Z_{1x}} & \frac{\partial H_3}{\partial Z_{1y}} & \frac{\partial H_3}{\partial Z_{2x}} & \frac{\partial H_3}{\partial Z_{2y}} & \frac{\partial H_3}{\partial Z_{4x}} & \frac{\partial H_3}{\partial Z_{4y}} & \frac{\partial H_3}{\partial t} \\ \frac{\partial H_4}{\partial Z_{1x}} & \frac{\partial H_4}{\partial Z_{1y}} & \frac{\partial H_4}{\partial Z_{2x}} & \frac{\partial H_4}{\partial Z_{2y}} & \frac{\partial H_4}{\partial Z_{4x}} & \frac{\partial H_4}{\partial Z_{4y}} & \frac{\partial H_4}{\partial t} \\ \frac{\partial H_5}{\partial Z_{1x}} & \frac{\partial H_5}{\partial Z_{1y}} & \frac{\partial H_5}{\partial Z_{2x}} & \frac{\partial H_5}{\partial Z_{2y}} & \frac{\partial H_5}{\partial Z_{4x}} & \frac{\partial H_5}{\partial Z_{4y}} & \frac{\partial H_5}{\partial t} \\ \frac{\partial H_6}{\partial Z_{1x}} & \frac{\partial H_6}{\partial Z_{1y}} & \frac{\partial H_6}{\partial Z_{2x}} & \frac{\partial H_6}{\partial Z_{2y}} & \frac{\partial H_1}{\partial Z_{4x}} & \frac{\partial H_6}{\partial Z_{4y}} & \frac{\partial H_6}{\partial t} \end{bmatrix}$$

The Jacobian matrix occupies the first six columns of the augmented matrix above. Factorization and inversion of the Jacobian followed by post-multiplication with the elements of column seven result in the derivatives of each undetermined parameter with respect to the homotopy parameter ($\frac{dZ_{1x}}{dt}, \frac{dZ_{1y}}{dt}, etc.$) The system modeled from the above matrix requires that the link parameters Z_{3x} and Z_{3y} be specified. However, the choice of Z_{3x} and Z_{3y} is not a necessity, and the matrix columns could be adjusted accordingly if two other choices for specified parameters were preferred. It should be noted that the choice of parameters to be specified may be dictated by design considerations and in some cases the degree of the system may be reduced through selective parameter specification.

The determinant of the augmented Jacobian, with the j^{th} column deleted, (where the parameter to be integrated resides in the j^{th} column), $|J_A|$, divided by the determinant of the Jacobian, $|J|$, provides the appropriate expression to be integrated with respect to the homotopy parameter. The sign of the integrand is given by $(-1)^{(j+1)}$. Symbolically,

$$\frac{dZ_j}{dt} = (-1)^{(j+1)} * \frac{|J_A|}{|J|} \tag{2.18}$$

Even though the homotopy functions are complex, integration can be performed separately on real and imaginary parts, and the results combined in complex form. The elements of the Jacobian were obtained analytically by differentiation of Eq.(2.15) rather than by using numerical estimates. At the end of the integration process Newton-Raphson iteration may be performed to refine values along the continuation path. Integration of Eq.(2.18) culminates in the synthesis of a four-bar mechanism passing through seven precision points.

CHAPTER 3. FIVE-BAR - SEVEN PRECISION POINTS

Similar to the target system of Eq. (2.15), development of the system of polynomial equations for the five-bar, seven precision point synthesis problem begins with loop closure equations. Elimination of parameters α_j and γ_j in Eq. (2.1) and expansion of resulting terms into real and imaginary parts, results in the target system of the five-bar synthesis algorithm,

$$\begin{aligned} F_j(Z_1, Z_2) &= 2A_{1j}sin\phi_j + 2(1 - cos\phi_j)B_{1j} + D_{1j} \\ F_{j+6}(Z_3, Z_4) &= 2A_{2j}sin\psi_j + 2(1 - cos\psi_j)B_{2j} + D_{2j} \end{aligned} \tag{3.1}$$

$A_{1j}, B_{1j}, D_{1j}, A_{2j}, B_{2j}$ and D_{2j} remain as defined in Eq.(2.12). The unknowns for the system are found to include:

1. The eight components of the mechanism's link dimensions, (Z_{1x}, Z_{1y},etc.)
2. The angular displacements of the input and output link (ϕ_j, ψ_j)
3. The gear ratio, GR.

We note that the ouput angular displacement, ψ_j, may be expressed as (Sandor and Erdman, 1984):

$$\psi_j = GR * \phi_j \tag{3.2}$$

Fourteen unknowns are involved, not counting the gear ratio which is allowed to vary over a range of values. The first two angular displacements of link Z_1 (ϕ_1, and ϕ_2), were also specified, resulting in 12 polynomial equations in 13 unknowns.

Morgan (1981) presented a numerical method whereby all real solutions to a system of N polynomial equations in N+1 unknowns may be found. Previously, in this presentation, the theoretically verified homotopy functions, represented by Eqs. (2.16) and (2.17) have been employed to find solutions. However the method described below *does not* implement either of these equations and resultingly, the method may prematurely fail. Nonetheless, a family of geared five-bar mechanisms will result even if the desired final gear ratio is not attained. The $N+1$ method requires determination of the system's Jacobian matrix augmented with the partial derivative of the target system with respect to the $Nth+1$ unknown ($\frac{\partial F_j}{\partial(N+1)}$).

The twelve equations noted in Eq. (3.1) represent the target system, F_j, and the $N+1$ parameter is, in this synthesis problem, the gear ratio, GR. Eq. (3.1) is in fact an intermediate expression developed by Subbian and Flugrad (1989). Algebraic manipulation and trigonometric substitutions to accomplish complete elimination of trigonometric terms was demonstrated in Chapter 2. However, the dependence of the output displacement, ψ_j on the input displacement, ϕ_j, is important to the synthesis of a geared five-bar linkage with gears fixed to links Z_1 and Z_4. Also, it was the intent of this development to preclude the constraint that the gear ratio be an integer value. As a result, further elimination of trigonometric functions through algebraic treatment, substitution, or series expansion was not possible.

The Jacobian matrix for the system of equations required for synthesis of a geared five-bar mechanism follows,

$$\begin{bmatrix}
\frac{\partial F_1}{\partial Z_{1x}} & \frac{\partial F_1}{\partial Z_{1y}} & \frac{\partial F_1}{\partial Z_{2x}} & \frac{\partial F_1}{\partial Z_{2y}} & \frac{\partial F_1}{\partial Z_{3x}} & \frac{\partial F_1}{\partial Z_{3y}} & \frac{\partial F_1}{\partial Z_{4x}} & \frac{\partial F_1}{\partial Z_{4y}} & \frac{\partial F_1}{\partial \phi_3} & \frac{\partial F_1}{\partial \phi_4} & \frac{\partial F_1}{\partial \phi_5} & \frac{\partial F_1}{\partial \phi_6} & \frac{\partial F_1}{\partial GR} \\
\frac{\partial F_2}{\partial Z_{1x}} & \frac{\partial F_2}{\partial Z_{1y}} & \frac{\partial F_2}{\partial Z_{2x}} & \frac{\partial F_2}{\partial Z_{2y}} & \frac{\partial F_2}{\partial Z_{3x}} & \frac{\partial F_2}{\partial Z_{3y}} & \frac{\partial F_2}{\partial Z_{4x}} & \frac{\partial F_2}{\partial Z_{4y}} & \frac{\partial F_2}{\partial \phi_3} & \frac{\partial F_2}{\partial \phi_4} & \frac{\partial F_2}{\partial \phi_5} & \frac{\partial F_2}{\partial \phi_6} & \frac{\partial F_2}{\partial GR} \\
\frac{\partial F_3}{\partial Z_{1x}} & \frac{\partial F_3}{\partial Z_{1y}} & \frac{\partial F_3}{\partial Z_{2x}} & \frac{\partial F_3}{\partial Z_{2y}} & \frac{\partial F_3}{\partial Z_{3x}} & \frac{\partial F_3}{\partial Z_{3y}} & \frac{\partial F_3}{\partial Z_{4x}} & \frac{\partial F_3}{\partial Z_{4y}} & \frac{\partial F_3}{\partial \phi_3} & \frac{\partial F_3}{\partial \phi_4} & \frac{\partial F_3}{\partial \phi_5} & \frac{\partial F_3}{\partial \phi_6} & \frac{\partial F_3}{\partial GR} \\
\frac{\partial F_4}{\partial Z_{1x}} & \frac{\partial F_4}{\partial Z_{1y}} & \frac{\partial F_4}{\partial Z_{2x}} & \frac{\partial F_4}{\partial Z_{2y}} & \frac{\partial F_4}{\partial Z_{3x}} & \frac{\partial F_4}{\partial Z_{3y}} & \frac{\partial F_4}{\partial Z_{4x}} & \frac{\partial F_4}{\partial Z_{4y}} & \frac{\partial F_4}{\partial \phi_3} & \frac{\partial F_4}{\partial \phi_4} & \frac{\partial F_4}{\partial \phi_5} & \frac{\partial F_4}{\partial \phi_6} & \frac{\partial F_4}{\partial GR} \\
\frac{\partial F_5}{\partial Z_{1x}} & \frac{\partial F_5}{\partial Z_{1y}} & \frac{\partial F_5}{\partial Z_{2x}} & \frac{\partial F_5}{\partial Z_{2y}} & \frac{\partial F_5}{\partial Z_{3x}} & \frac{\partial F_5}{\partial Z_{3y}} & \frac{\partial F_5}{\partial Z_{4x}} & \frac{\partial F_5}{\partial Z_{4y}} & \frac{\partial F_5}{\partial \phi_3} & \frac{\partial F_5}{\partial \phi_4} & \frac{\partial F_5}{\partial \phi_5} & \frac{\partial F_5}{\partial \phi_6} & \frac{\partial F_5}{\partial GR} \\
\frac{\partial F_6}{\partial Z_{1x}} & \frac{\partial F_6}{\partial Z_{1y}} & \frac{\partial F_6}{\partial Z_{2x}} & \frac{\partial F_6}{\partial Z_{2y}} & \frac{\partial F_6}{\partial Z_{3x}} & \frac{\partial F_6}{\partial Z_{3y}} & \frac{\partial F_6}{\partial Z_{4x}} & \frac{\partial F_6}{\partial Z_{4y}} & \frac{\partial F_6}{\partial \phi_3} & \frac{\partial F_6}{\partial \phi_4} & \frac{\partial F_6}{\partial \phi_5} & \frac{\partial F_6}{\partial \phi_6} & \frac{\partial F_6}{\partial GR} \\
\frac{\partial F_7}{\partial Z_{1x}} & \frac{\partial F_7}{\partial Z_{1y}} & \frac{\partial F_7}{\partial Z_{2x}} & \frac{\partial F_7}{\partial Z_{2y}} & \frac{\partial F_7}{\partial Z_{3x}} & \frac{\partial F_7}{\partial Z_{3y}} & \frac{\partial F_7}{\partial Z_{4x}} & \frac{\partial F_7}{\partial Z_{4y}} & \frac{\partial F_7}{\partial \phi_3} & \frac{\partial F_7}{\partial \phi_4} & \frac{\partial F_7}{\partial \phi_5} & \frac{\partial F_7}{\partial \phi_6} & \frac{\partial F_7}{\partial GR} \\
\frac{\partial F_8}{\partial Z_{1x}} & \frac{\partial F_8}{\partial Z_{1y}} & \frac{\partial F_8}{\partial Z_{2x}} & \frac{\partial F_8}{\partial Z_{2y}} & \frac{\partial F_8}{\partial Z_{3x}} & \frac{\partial F_8}{\partial Z_{3y}} & \frac{\partial F_8}{\partial Z_{4x}} & \frac{\partial F_8}{\partial Z_{4y}} & \frac{\partial F_8}{\partial \phi_3} & \frac{\partial F_8}{\partial \phi_4} & \frac{\partial F_8}{\partial \phi_5} & \frac{\partial F_8}{\partial \phi_6} & \frac{\partial F_8}{\partial GR} \\
\frac{\partial F_9}{\partial Z_{1x}} & \frac{\partial F_9}{\partial Z_{1y}} & \frac{\partial F_9}{\partial Z_{2x}} & \frac{\partial F_9}{\partial Z_{2y}} & \frac{\partial F_9}{\partial Z_{3x}} & \frac{\partial F_9}{\partial Z_{3y}} & \frac{\partial F_9}{\partial Z_{4x}} & \frac{\partial F_9}{\partial Z_{4y}} & \frac{\partial F_9}{\partial \phi_3} & \frac{\partial F_9}{\partial \phi_4} & \frac{\partial F_9}{\partial \phi_5} & \frac{\partial F_9}{\partial \phi_6} & \frac{\partial F_9}{\partial GR} \\
\frac{\partial F_{10}}{\partial Z_{1x}} & \frac{\partial F_{10}}{\partial Z_{1y}} & \frac{\partial F_{10}}{\partial Z_{2x}} & \frac{\partial F_{10}}{\partial Z_{2y}} & \frac{\partial F_{10}}{\partial Z_{3x}} & \frac{\partial F_{10}}{\partial Z_{3y}} & \frac{\partial F_{10}}{\partial Z_{4x}} & \frac{\partial F_{10}}{\partial Z_{4y}} & \frac{\partial F_{10}}{\partial \phi_3} & \frac{\partial F_{10}}{\partial \phi_4} & \frac{\partial F_{10}}{\partial \phi_5} & \frac{\partial F_{10}}{\partial \phi_6} & \frac{\partial F_{10}}{\partial GR} \\
\frac{\partial F_{11}}{\partial Z_{1x}} & \frac{\partial F_{11}}{\partial Z_{1y}} & \frac{\partial F_{11}}{\partial Z_{2x}} & \frac{\partial F_{11}}{\partial Z_{2y}} & \frac{\partial F_{11}}{\partial Z_{3x}} & \frac{\partial F_{11}}{\partial Z_{3y}} & \frac{\partial F_{11}}{\partial Z_{4x}} & \frac{\partial F_{11}}{\partial Z_{4y}} & \frac{\partial F_{11}}{\partial \phi_3} & \frac{\partial F_{11}}{\partial \phi_4} & \frac{\partial F_{11}}{\partial \phi_5} & \frac{\partial F_{11}}{\partial \phi_6} & \frac{\partial F_{11}}{\partial GR} \\
\frac{\partial F_{12}}{\partial Z_{1x}} & \frac{\partial F_{12}}{\partial Z_{1y}} & \frac{\partial F_{12}}{\partial Z_{2x}} & \frac{\partial F_{12}}{\partial Z_{2y}} & \frac{\partial F_{12}}{\partial Z_{3x}} & \frac{\partial F_{12}}{\partial Z_{3y}} & \frac{\partial F_{12}}{\partial Z_{4x}} & \frac{\partial F_{12}}{\partial Z_{4y}} & \frac{\partial F_{12}}{\partial \phi_3} & \frac{\partial F_{12}}{\partial \phi_4} & \frac{\partial F_{12}}{\partial \phi_5} & \frac{\partial F_{12}}{\partial \phi_6} & \frac{\partial F_{12}}{\partial GR}
\end{bmatrix}$$

For each dyad, one equation results per displacement, j. Consequently, for the seven precision point synthesis problem, 12 equations adequately model the system. The augmented Jacobian dimension is 12 rows by 13 columns; the first six rows are a consequence of the movement of dyad 1; the remaining rows are a consequence of the movement of dyad 2.

As shown before, derivatives are acquired through evaluation of the Jacobian's determinant, $\left|J_{(N+1)}\right|$, as well as the determinant of the augmented matrix, $\left|J_{A(N+1)}\right|$, with the *kth* column deleted followed by division of the determinants. Subsequent integration of these terms leads to the determination of the unknown parameters. The integrand's sign is determined by the coefficient $(-1)^{(k+1)}$.

$$\frac{dZ_k}{d(GR)} = (-1)^{(k+1)} * \frac{\left|J_{A(N+1)}\right|}{\left|J_{(N+1)}\right|} \tag{3.3}$$

Integration begins with a lower limit of unity since the start system's gear ratio will always be +1.0. This conclusion results from the fact that the start system is found by implementing Robert's theorem. Robert's theorem provides three five-bar

cognates with gear ratio $+1.0$ from a single parent four-bar. (Synthesis equations for a four-bar passing through seven precision points using continuation were developed in the preceding section.) When the upper limit of integration is reached, the designer has a solution set of geared five-bar linkages over a range of varying gear ratios. The upper limit of integration is limited by the physical constraints of the linkage. For instance, if integration is performed from a starting gear ratio of $+1.0$ to a final gear ratio of -1.0, a singularity occurs at a gear ratio of 0.0. The effect of gear ratios approaching zero is manifested in some link parameters approaching infinity. The significance of this numerical proclivity is realized physically in the synthesis of a rack mechanism. Figure 3.1 depicts a rack device in which the magnitude of link Z_3 is much greater than the magnitude of link Z_4. In this instance $Z_3's$ magnitude approaches an infinite length.

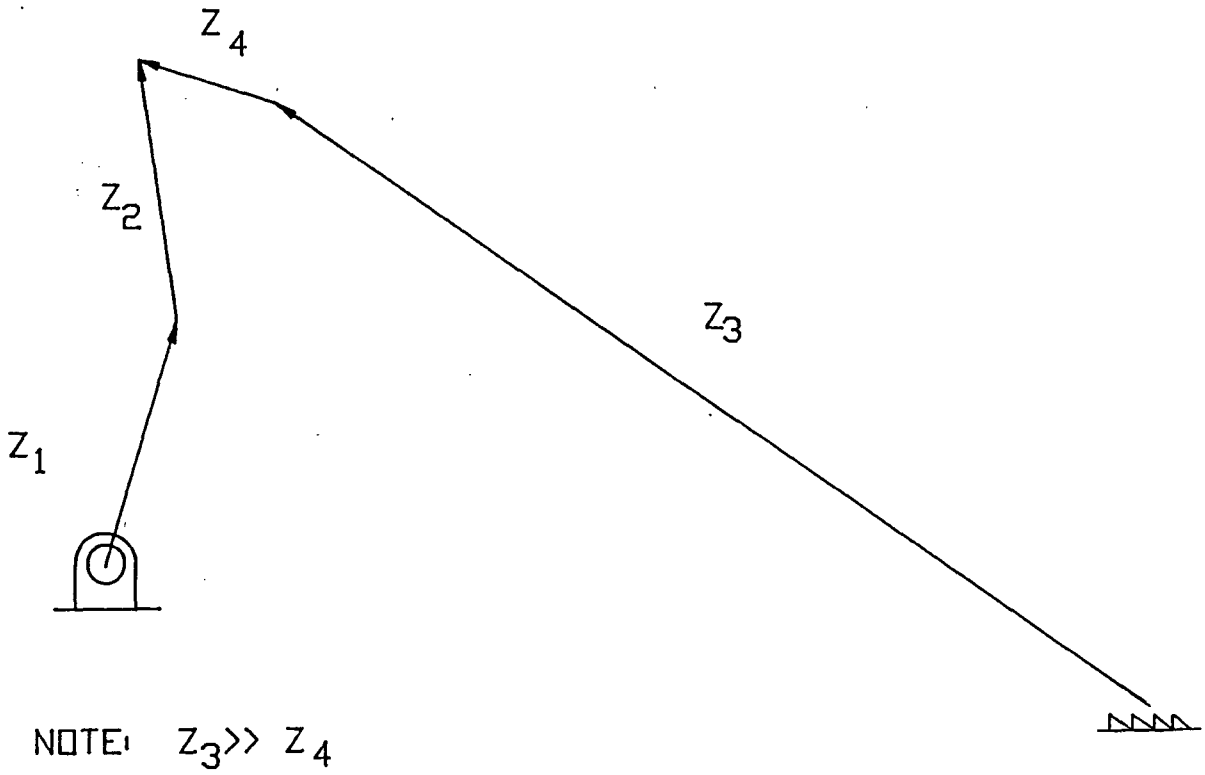

Figure 3.1: Rack mechanism

CHAPTER 4. ALTERNATE GEAR CONFIGURATIONS

The synthesis of a geared five-bar mechanism with gears configured as noted in Figure 4.1 may be accomplished through continuation methods similar to those developed in Chapter 3. However, the equations of synthesis for geared five-bar mechanisms with gears held fixed to a stationary link are considerably easier to solve with continuation than mechanisms with a configuration like those shown in Figures 4.1 and 4.2. The requirement that the equations of synthesis be expressed in polynomial form, as well as the enforcement of the gearing relationship at every integration step complicates the synthesis for the case where the ground link is not the intermediate link between gears. For example, Figure 4.2 depicts a geared mechanism where the angular displacement of link $\mathbf{Z_2}$ is a function of angular displacements in link **A**, (γ_j), and link $\mathbf{Z_1}$, (ϕ_j). Closed form solutions for angular displacements ψ_j and γ_j of dyad componets $\mathbf{Z_4}$ and **B**, respectively, may be written through application of inverse kinematics (see Appendix A). Consequently, selection of the mechanism's precision points as well as magnitudes and the initial orientation of link components $\mathbf{Z_4}$ and **B**, result in the angular displacements ψ_j and γ_j required to pass through the specified points. Then synthesis of triad $\mathbf{Z_1} - \mathbf{Z_2} - \mathbf{A}$ is accomplished through continuation. The loop closure equation for the triad given by,

$$\mathbf{Z_1}(e^{i\phi_j} - 1) + \mathbf{Z_2}(e^{i\alpha_j} - 1) + \mathbf{A}(e^{i\gamma_j} - 1) \;=\; 0 \qquad (4.1)$$

The equations of synthesis for the triad are as follows:

$$
\begin{aligned}
&REAL: \\
&\delta_{xj} = Z_{1x}cos\phi_j - Z_{1x} - Z_{1y}sin\phi_j + Z_{2x}cos\alpha_j \\
&\quad - Z_{2y}sin\alpha_j + A_xcos\gamma_j - Z_{2x} - A_x - A_ysin\gamma_j \\
&IMAGINARY: \\
&\delta_{yj} = Z_{1y}cos\phi_j - Z_{1y} + Z_{1x}sin\phi_j + Z_{2y}cos\alpha_j \\
&\quad + Z_{2x}sin\alpha_j + A_ycos\gamma_j - Z_{2y} - A_y + A_xsin\gamma_j \qquad (4.2)
\end{aligned}
$$

The gearing relationship between the coupler link ($A - B - Z_3$) and links Z_1 and Z_2 must be enforced through the following equation,

$$\gamma_j = \alpha_j + \left[\alpha_j - \phi_j\right] GR \qquad (4.3)$$

Solving for α_j, we have,

$$\alpha_j = \frac{\gamma_j + GR * \phi_j}{1 + GR} \qquad (4.4)$$

Substitution for α_j into Eq.(4.1), and implementation of trigonometric identities for sine and cosine terms yields,

$$
\begin{aligned}
\delta_{xj} &= Z_{1x}cos\phi_j - Z_{1x} - Z_{1y}sin\phi_j - Z_{2x} - A_x + A_xcos\gamma_j - A_ysin\gamma_j \\
&+ Z_{2x}\left[cos(\frac{\gamma_j}{1+GR})cos(\frac{\phi_jGR}{1+GR}) - sin(\frac{\gamma_j}{1+GR})sin(\frac{\phi_jGR}{1+GR})\right] \\
&- Z_{2y}\left[cos(\frac{\gamma_j}{1+GR})cos(\frac{\phi_jGR}{1+GR}) - sin(\frac{\gamma_j}{1+GR})sin(\frac{\phi_jGR}{1+GR})\right] \\
\delta_{yj} &= Z_{1y}cos\phi_j - Z_{1y} + Z_{1x}sin\phi_j + A_ycos\gamma_j - Z_{2y} - A_y + A_xsin\gamma_j \\
&+ Z_{2y}\left[cos(\frac{\gamma_j}{1+GR})cos(\frac{\phi_jGR}{1+GR}) - sin(\frac{\gamma_j}{1+GR})sin(\frac{\phi_jGR}{1+GR})\right] \\
&+ Z_{2x}\left[cos\frac{\gamma_j}{1+GR}cos\frac{\phi_jGR}{1+GR} - sin\frac{\gamma_j}{1+GR}sin\frac{\phi_jGR}{1+GR}\right]
\end{aligned}
\qquad (4.5)
$$

The list of unknowns for this system of equations includes Z_{1x}, Z_{1y}, Z_{2x}, Z_{2y}, A_x, A_y, and $cos(\frac{\phi_j GR}{1+GR})$ and $sin(\frac{\phi_j GR}{1+GR})$ for each of the six displacements. The $cos(\frac{\phi_j GR}{1+GR})$ and $sin(\frac{\phi_j GR}{1+GR})$ terms are treated as separate variables due to the fact that continuation methods require expressions in polynomial form. Thus, the identity $cos^2(\frac{\phi_j GR}{1+GR})+sin^2(\frac{\phi_j GR}{1+GR}) = 1$ must be enforced at every step - adding one equation to the two synthesis equations at every precision point. Table 4.1 notes the number of unknowns, number of equations and required number of specified parameters for each of the seven precision points.

Table 4.1: Summary of unknowns and equations for mechanism in Figure 4.2

Position	Displacement	No. Unknowns	No. Equations	No. Specified Parameters
2	1	8	3	5
3	2	10	6	4
4	3	12	9	3
5	4	14	12	2
6	5	16	15	1
7	6	18	18	0

For each displacement of the triad, two unknowns, $cos(\frac{\phi_j GR}{1+GR})$ and $sin(\frac{\phi_j GR}{1+GR})$ are added. The real and imaginary components of the triad's synthesis equations in addition to the trigonometric identity $cos^2(\frac{\phi_j GR}{1+GR}) + sin^2(\frac{\phi_j GR}{1+GR}) = 1$ add three equations with every displacement. Examination of the equations of synthesis indicates that the degree of each synthesis equation is of order two as is the trig identity. Bezout's theorem (Version 2, as stated by Morgan (1987)) indicates that:

1. unless a system has an infinite number of solutions, the number of its solutions is less than or equal to its total degree.

2. unless a system has an infinite number of solutions or an infinite number

of solutions at infinity, the number of its solutions at infinity adds up to exatly the total degree, counting multiplicities

The degree of each polynomial in this instance is of order 2. A total of eighteen equations result, including the equations enforcing the trigonometric identities, therefore, by invoking Bezout's theorem it can be predicted that 2^{18} or 262,144 solutions to the system of equations exist. Tracking each of the 262,144 paths predicted by Bezout's theorem in continuation would require considerable computer time. The seemingly innocuous substitution of the gearing relationship in the equations of synthesis for the configuration shown in Figure 4.2 renders the synthesis of this particular mechanism relatively intractable. However, by modifying the mechanism's gearing, continuation methods may be implemented to design a triad that can be combined with a dyad to produce a geared five-bar solution set over a range of gear ratios. Figure 4.1 depicts the mechanism of interest. The gearing relationship for this device is:

$$\alpha_j = \gamma_j + \left[\gamma_j - \psi_j\right] * GR \tag{4.6}$$

Notably, the angular displacement of triad component Z_1 which is ϕ_j, does not appear in the gearing equation. Consequently, ϕ_j can be eliminated from the equations of synthesis in the following manner:

1. The real component of Eq. (4.1) is multiplied by Z_{1y}; the imaginary part is multiplied by Z_{1x} and the resulting products are subtracted. This produces an expression for $sin\phi_j$.
2. Then the real part of of Eq. (4.1) is multiplied by Z_{1x} while the imaginary component is multiplied by Z_{1y}. These are added to develop an expression for $cos\phi_j$.

3. The results from (1) and (2) are substituted into $sin^2\phi_j + cos^2\phi_j = 1$ to finally eliminate $sin\phi_j$ and $cos\phi_j$.

This process leads to the following expression,

$$2A_j sin\alpha_j + 2(1 - cos\alpha_j)B_j + D_j = 0 \tag{4.7}$$

where:

$$\begin{aligned}
A_j &= Z_{1x}Z_{2y} - Z_{1y}Z_{2x} + Z_{2y}\delta_{xj} - Z_{2x}\delta_{yj} \\
&+ (cos\gamma_j - 1)(Z_{2x}A_y - Z_{2y}A_x) + sin\gamma_j(Z_{2y}A_y + Z_{2x}A_x) \\
B_j &= Z_{2x}^2 + Z_{2y}^2 + Z_{2x}Z_{1x} + Z_{1y}Z_{2y} + Z_{2y}\delta_{yj} + Z_{2x}\delta_{xj} \\
&+ sin\gamma_j(Z_{2x}A_y - Z_{2y}A_x) + (cos\gamma_j - 1)(-Z_{2x}A_x - Z_{2y}A_y) \\
D_j &= 2(Z_{1x}\delta_{xj} + Z_{1y}\delta_{yj}) + \delta_{xj}^2 + \delta_{yj}^2 \\
&- 2(cos\gamma_j - 1)\left[Z_{1x}A_x + Z_{1y}A_y + A_x\delta_{xj} + A_y\delta_{yj} + A_x^2 + A_y^2\right]
\end{aligned} \tag{4.8}$$

Substitution of the gearing relationship of Eq. (4.5) into Eq. (4.6) gives,

$$2A_j sin(\gamma_j + (\gamma_j - \psi_j)GR) + 2\left[(1 - cos(\gamma_j + (\gamma_j - \psi_j)GR)\right]B_j + D_j = 0 \tag{4.9}$$

The unknowns in this system are Z_{1x}, Z_{1y}, A_x, A_y, Z_{2x}, Z_{2y}, and GR. Since GR is the independent variable of integration, and the angular displacements γ_j and ψ_j are known, the trigonometric terms appearing in Eq. (4.8) need not be treated as independent variables. Table 4.2 lists the number of unknowns and available equations with each displacement.

Solutions of a generic system with a gearing configuration like that shown in Figure 4.1 would require the solution of six second order equations, with one parameter-the gear ratio-being specified. Continuation would then track 2^6 or 64 paths to all

existing solutions - real, complex, and infinite. However, a solution set of five-bars can be found over a range of gear ratios by implementing the $N + 1$ method detailed in Chapter 3. Eq. (4.8) is differentiated with respect to each of the unknown parameters yielding a (6 X 7) augmented Jacobian matrix.

Table 4.2: Summary of unknowns and equations for mechanism in Figure 4.1

Position	Displacement	No. Unknowns	No. Equations	No. Specified Parameters
2	1	7	1	6
3	2	7	2	5
4	3	7	3	4
5	4	7	4	3
6	5	7	5	2
7	6	7	6	1

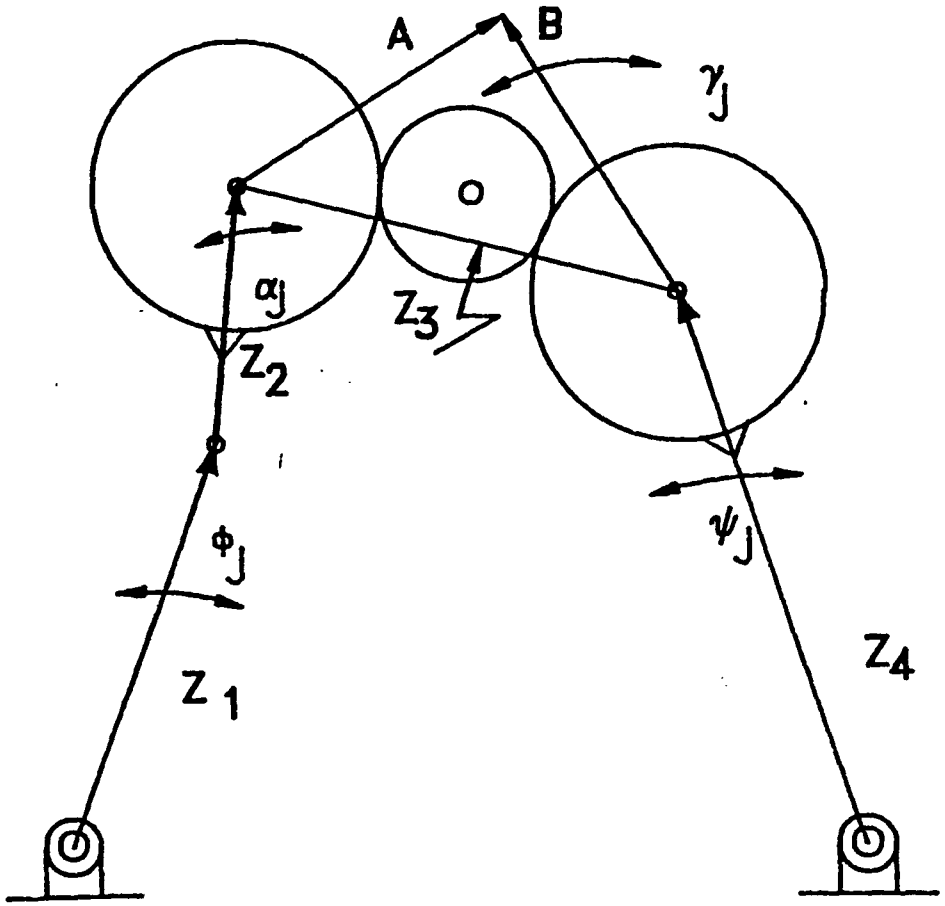

Figure 4.1: Alternate gear configuration 1

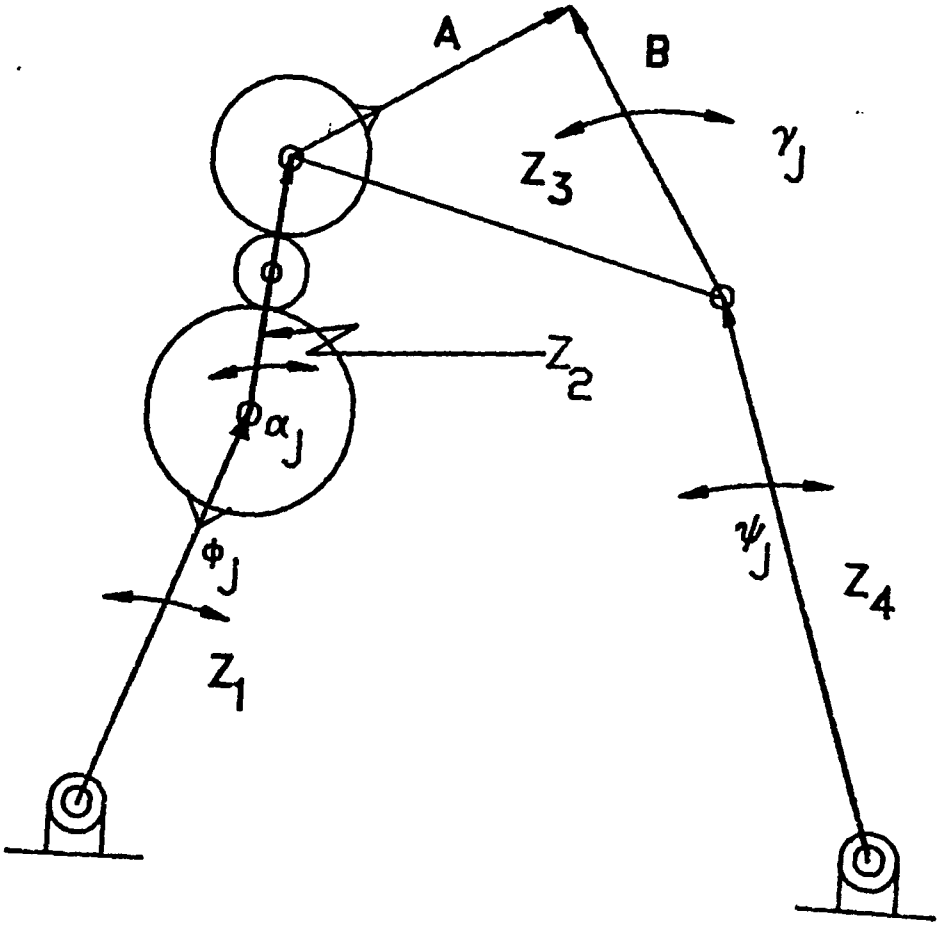

Figure 4.2: Alternate gear configuration 2

CHAPTER 5. SYNTHESIS EXAMPLES

All numerical procedures described below were performed on a VAX/VMS 11/785 central processing unit using VAX FORTRAN and supported at the ANSI FORTRAN-77 level. The GEAR method of integration was implemented for all integration procedures; integration step size was no larger than $1.0E-6$ for all examples.

Example 1 begins with a four-bar mechanism passing through the five precision points noted in Table 5.1. Implementation of Eq. (2.17), previously referred to as the modified homotopy function, results in the addition of two more precision points to the coupler path. The target system, $F(Z_j)$ contains the values of the coupler points that the final design is required to pass through. The start system, $G(Z_j)$, is equal in value to the target system for the five original precision points. However, the remaining two start functions contain the points on the original four-bar's coupler curve that are closest in magnitude, direction and timing to the two new points. As the homotopy parameter, t, approaches 1, the value of the homotopy function becomes closer and closer in value to the target system. More succintly, the original path "moves toward" the new path. Figure 5.1 depicts the original four-bar passing through the five initially specified precision points. The coupler path of the newly synthesized linkage is likewise shown passing through the original five points in addition to points 6 and 7. Table 5.1 lists the five original coupler points and

Table 5.2 notes the two new points. In this particular example the newly prescribed precision points were selected to follow positions four and five. However, this choice is arbitrary as long as timing and proximity criteria are observed. Figure 5.2 shows the new four-bar mechanism (links $\mathbf{Z_1} - \mathbf{Z_2} - \mathbf{Z_3} - \mathbf{Z_4}$) and one of its three five-bar cognates (links $\mathbf{Z_1'} - \mathbf{Z_2'} - \mathbf{Z_3'} - \mathbf{Z_4'}$) given by Robert's theorem. The numerical procedure required 15.81 CPU seconds to transform the four-bar mechanism passing through five precision points into a four-bar passing through seven precision points. From this theorem we know that a geared five-bar cognate with gear ratio of +1.0 will trace the same coupler path as the parent four-bar. This knowledge enables the designer to identify a start system for the $N+1$ method detailed by Morgan (1981). As the gear ratio varies from +1.0 to its specified upper limit, the change in the mechanism can be documented graphically. It should be noted here that an "upper limit" may also imply integration of parameters beginning with +1.0 to values less than 0.0. As noted at the close of Chapter 2, gear ratios approaching zero, may result in the synthesis of mechanisms consisting of infinite link dimensions. At a gear ratio of 0.0 the value of the augmented Jacobian's determinant becomes singular, consequently the implementation of $N+1$ should include measures to preclude gear ratios equal to 0.0 but nonetheless capable of including negative values. Figure 5.3 shows the change in the links of the original five-bar mechanism with a range of gear ratios. On the dependent axes, link lengths and their respective orientations are plotted against the gear ratio. The $N+1$ method took 250.33 CPU seconds to construct the solution set of geared five-bar mechanisms over a range of gear ratios from +1.0 to +2.0.

Any geared five-bar selected from the solution set will pass through the precision

points specified in Tables 5.1 and 5.2. The validity of the results may be confirmed by substitution of appropriate values of the gear ratio and link parameters into Eq. (3.1). Figure 5.4 depicts the coupler path of the geared five-bar linkage selected from the solution set of five-bars at a gear ratio of +1.99.

Table 5.1: Original precision points for four-bar mechanism of Example 1

Precision Point	δ_x	δ_y
1	0.0000	0.0000
2	-0.4535	-0.1730
3	-0.8385	-0.5228
4	-1.0840	-0.9358
5	-1.1794	-1.2957

Table 5.2: New precision points for four-bar mechanism of Example 1

Precision Point	δ_x	δ_y
6	-1.1800	-1.3400
7	-1.0000	-1.6100

Table 5.3 summarizes the progression of a four-bar mechanism passing through five precision points to a geared five-bar with varying gear ratio passing through seven precision points.

Table 5.3: Progression of mechanism synthesis for Example 1

MECHANISM	Z_{1x}	Z_{1y}	Z_{2x}	Z_{2y}	Z_{3x}	Z_{3y}	Z_{4x}	Z_{4y}
4-BAR	0.0009	0.9997	1.1344	1.3975	-1.7287	0.5016	-0.6386	1.8974
NEW 4-BAR	0.0179	1.0364	1.1712	1.1432	-1.7287	0.5016	-0.7114	1.9475
5-BAR(1.00)	1.1712	1.1432	0.0179	1.0364	-0.7114	1.9475	-1.7287	0.5016
5-BAR(1.99)	1.7970	1.1693	0.0020	1.0347	-0.5379	1.7302	-0.6309	0.2106

Example 2 also illustrates the solution to the five-bar, seven precision point synthesis problem. The original four-bar mechanism generates the coupler path depicted in Figure

5.5 and is shown relative to the new linkage's path. Precision points that include those listed in Table 5.4, plus two additional points away from the line and noted in Table 5.5, were included in the target system. The start system includes the values of the original five precision points and the values of the points nearest in timing, magnitude, and direction on the original coupler path to the two new points on the resulting mechanism's curve. Figure 5.6 notes the Robert's five-bar cognate relative to the four-bar synthesized with the modified homotopy algorithm. The four-bar mechanism is made up of links $\mathbf{Z_1} - \mathbf{Z_2} - \mathbf{Z_3} - \mathbf{Z_4}$ and the five-bar cognate's links are $\mathbf{Z'_1} - \mathbf{Z'_2} - \mathbf{Z'_3} - \mathbf{Z'_4}$. This continuation procedure required 10.2 seconds of CPU time to produce the new four-bar mechanism. Figure 5.7 notes the change in the starting five-bar with gear ratio. Finally, Figure 5.8 shows the coupler path generated by a five-bar selected from the synthesis solution set. Integration from a gear ratio +1.0 to one of +1.3 required 275.33 seconds of CPU time. Table 5.6 notes the progression of synthesis-beginning with a four-bar passing through five precision points and culminating in a five-bar passing through seven precision points with a gear ratio equal to +1.25.

Table 5.4: Original precision points for four-bar mechanism of Example 2

Precision Point	δ_x	δ_y
1	0.0	0.0
2	-0.3	0.0
3	-0.6	0.0
4	-0.9	0.0
5	-1.2	0.0

Table 5.5: New precision points for four-bar mechanism of Example 2

Precision Point	δ_x	δ_y
6	1.35	0.15
7	1.25	0.18

Example 3 demonstrates the design procedure for incorporating a dyad passing through

Table 5.6: Progression of mechanism synthesis for Example 2

MECHANISM	Z_{1x}	Z_{1y}	Z_{2x}	Z_{2y}	Z_{3x}	Z_{3y}	Z_{4x}	Z_{4y}
4-BAR	-4.4669	5.0802	0.9723	0.2172	0.2572	1.7531	5.5340	-0.4733 .
NEW 4-BAR	-4.0311	3.8192	1.0413	0.2612	0.2572	1.7531	5.2111	-0.4109
5-BAR(1.00)	1.0413	0.2612	-4.0311	3.8192	5.2111	-0.4109	0.2572	1.7531
5-BAR(1.25)	0.6281	0.1574	-0.8429	0.2092	-0.5677	-0.8353	1.5244	0.2236

seven precision points and a triad synthesized through continuation and passing through the same seven points. As noted in Figure 4.1 the gearing configuration consists of a gear fastened to the intermediate link of the triad, $\mathbf{Z_2}$, as well as to the input link of the dyad, $\mathbf{Z_4}$. The link intermediate to these links is the coupler link, $\mathbf{A - B - Z_3}$.

The start mechanism's parameters are noted in Table 5.7 and were established from the algorithm developed by Subbian and Flugrad (1990) in their presentation on triad synthesis. A closed form solution was used to acquire values of the angular displacments of links $\mathbf{Z_4}$ and $\mathbf{B}$ noted in Table 5.8. Table 5.9 lists the coordinates of the precision points relative to the initial position of the linkage. Eq. (4.2) was implemented to solve for the angular displacement of link $\mathbf{Z_2}$, α_j, and subsequently the gear ratio, GR, was found by using Eq. (4.5). Displacements γ_j and ψ_j are known by implementation of inverse kinematics (see Appendix A). The solution for GR in Eq.(4.6) provides the lower limit of integration for the following system of equations:

$$\int_{GRSTART}^{GREND} \frac{dZ_j}{dGR}\, dGR \;=\; Z_j \tag{5.1}$$

Figure 5.9 shows the changes in parameters associated with the triad for the changing gear ratio. Figure 5.10 depicts the behavior of a geared five-bar mechanism chosen from the solution set and having a gear ratio of +1.2548. The procedure required 74.32 CPU seconds to establish the solution set of triads varying in gear ratio from 0.0 to +1.5. The coupler curve of the new mechanism is determined iteratively because the angular displacement of the triad's input link, $\mathbf{Z_1}$, is unknown and indeterminant from the gearing relationship.

Since the input angle of link $\mathbf{Z_1}$ was eliminated in the equations of synthesis, the mechanism that results is not functionally related to the angular displacement, ϕ_j, of link $\mathbf{Z_1}$. The analysis algorithm which finds the coupler path of the five-bar mechanism resulting from triad synthesis and kinematic inversion relies on the angular orientation of the driven link. The analysis routine requires that a link be driven a full cycle (360°) to adequately determine the behavior of the mechanism and its coupler curve. To accurately describe the path generated by the five-bar with a gear configuration as shown in Figure 4.1, the gearing relationship must be enforced along the entire path, in addition to the equations of analysis. At any given point along the coupler path the unknowns in the analysis procedure are ϕ_j, ψ_j, α_j, and γ_j. At each position of the coupler point, there are at most three equations; one of which ensures that $\alpha_j = \gamma_j + [\gamma_j - \psi_j] * GR$. The analysis for this particular design procedure requires iterative solution methods to find the mechanism's coupler path. Analysis methods for all mechanisms presented in this chapter are noted in Appendix B.

Table 5.7: Start mechanism parameters - Example 3

Z_1	Θ_1 (Degrees)	Z_2	Θ_2 (Degrees)	A	Θ_A (Degrees)
41.3970	356.0089	3.7906	84.5901	5.8867	351.8026

Table 5.8: Angular displacements - dyad - Example 3

Position	γ_j (Degrees)	ψ_j (Degrees)
1	14.8964	- 2.0473
2	28.0787	- 8.9064
3	37.9732	-20.7095
4	43.6838	-29.2973
5	50.4121	-36.9822
6	57.9338	-43.5473

Table 5.9: Precision points for five-bar mechanism of Example 3

Precision Point	δ_x	δ_y
1	0.0000	0.0000
2	-0.4019	1.5000
3	-1.5000	2.5981
4	-3.0000	3.0000
5	-4.0000	3.0000
6	-5.0000	3.0000
7	-6.0000	3.0000

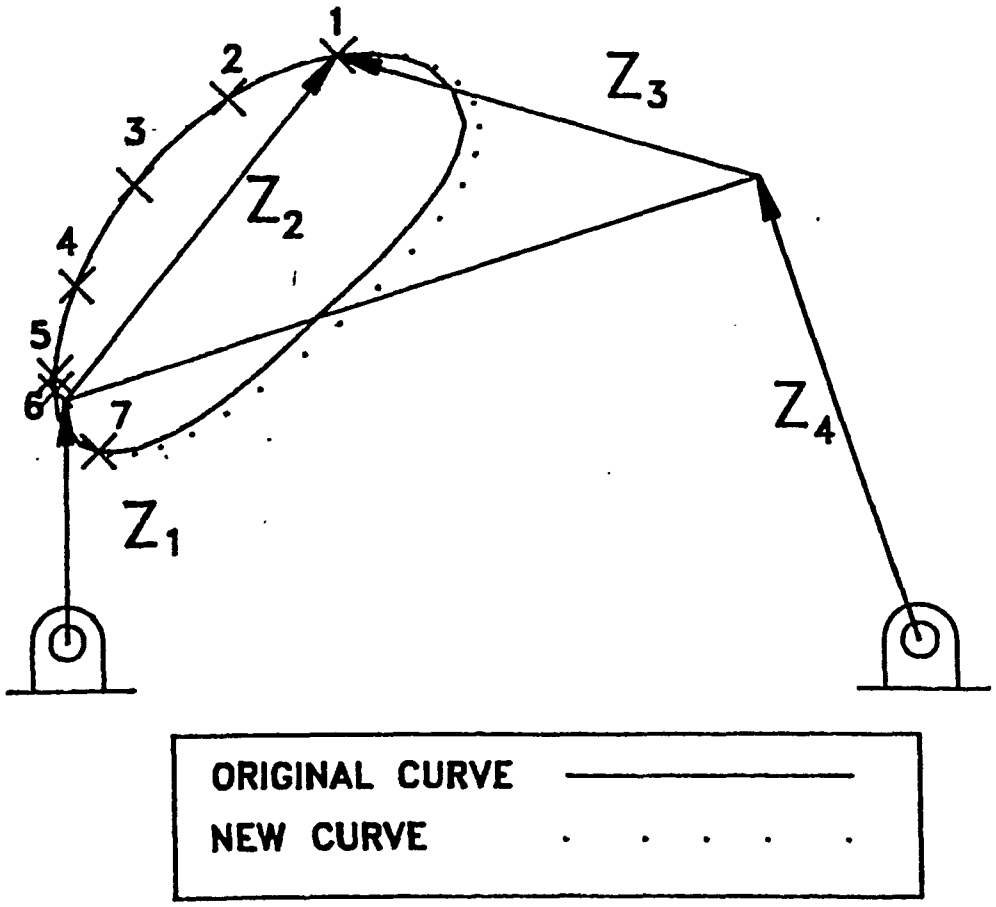

Figure 5.1: Original four-bar and coupler curve (Example 1)

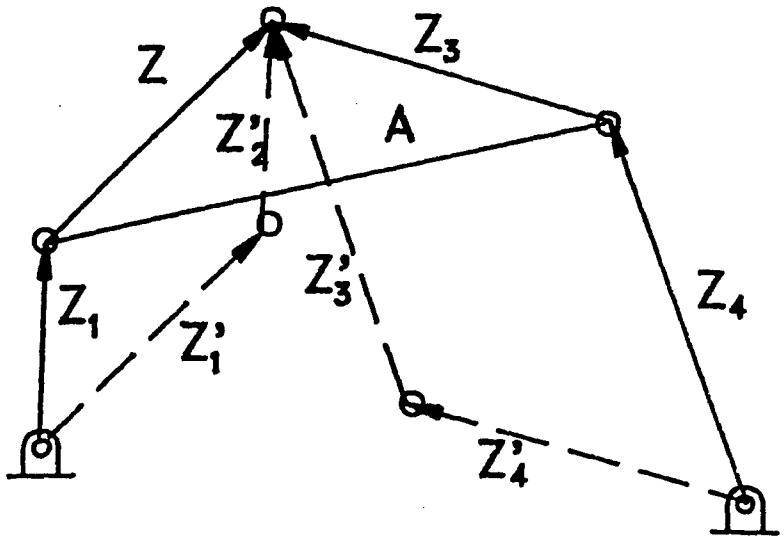

Figure 5.2: New four-bar and Robert's cognate (Example 1)

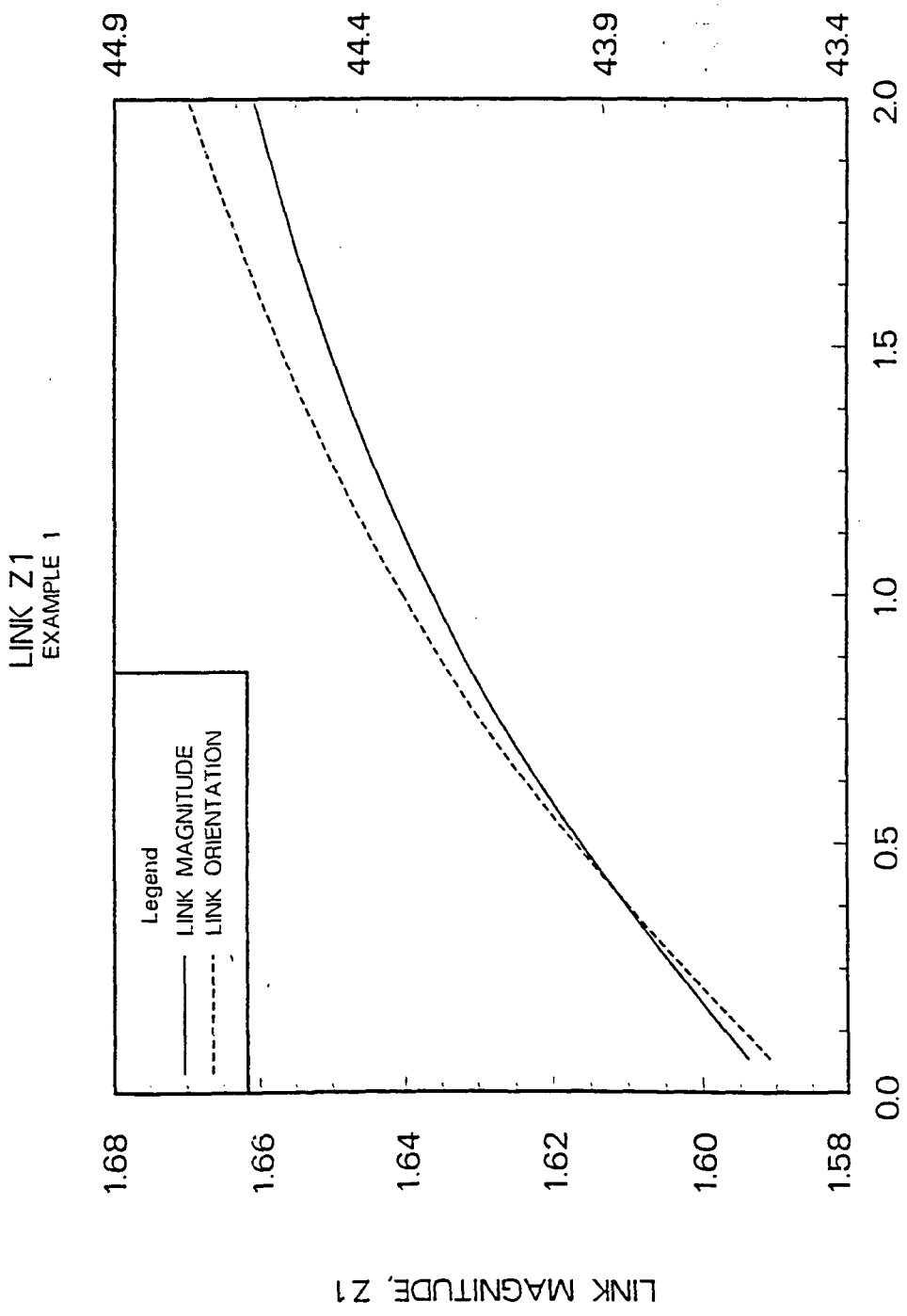

Figure 5.3: Link magnitudes and orientations with changing gear ratio (Example 1)

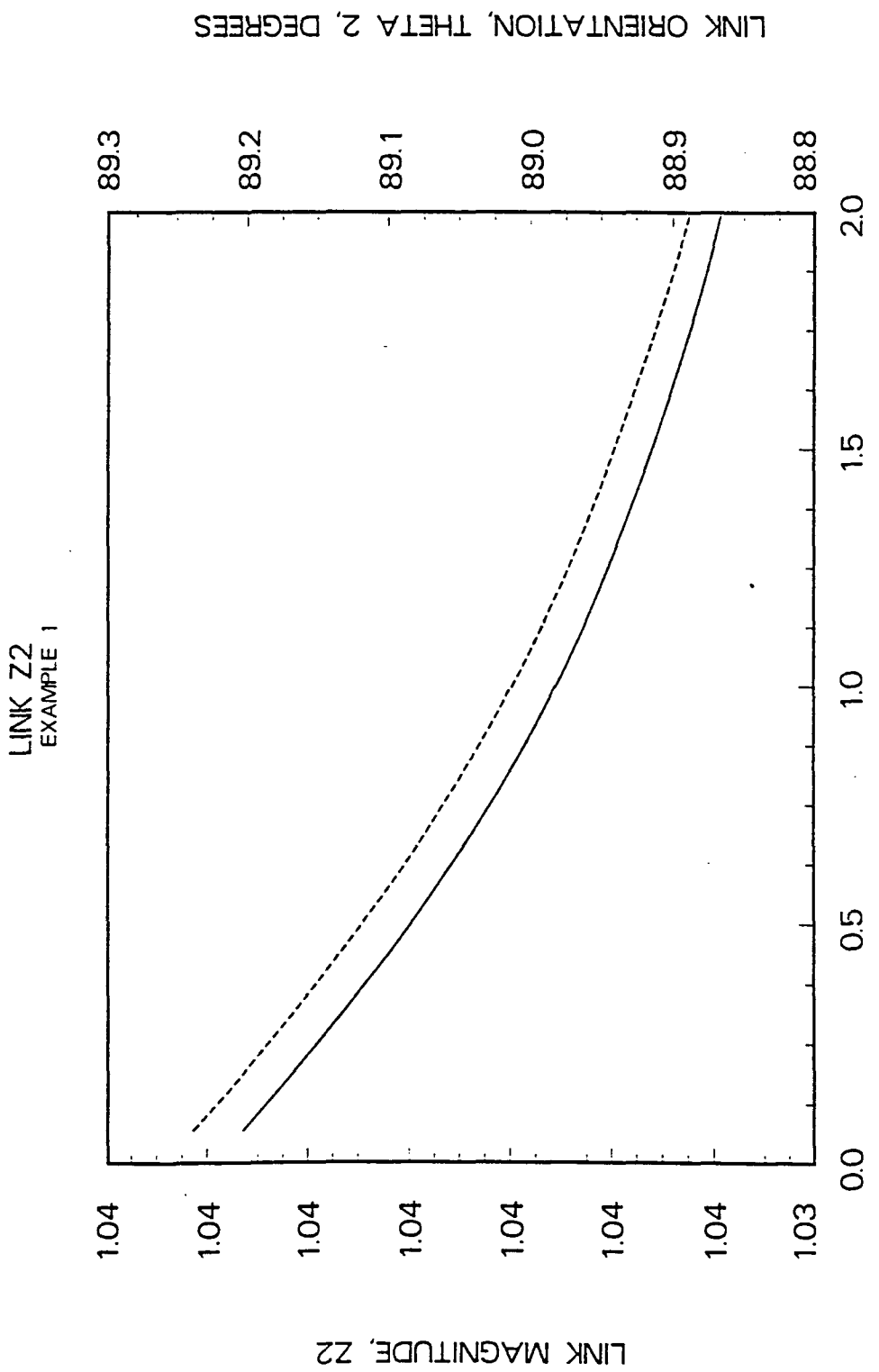

Figure 5.3 (Continued)

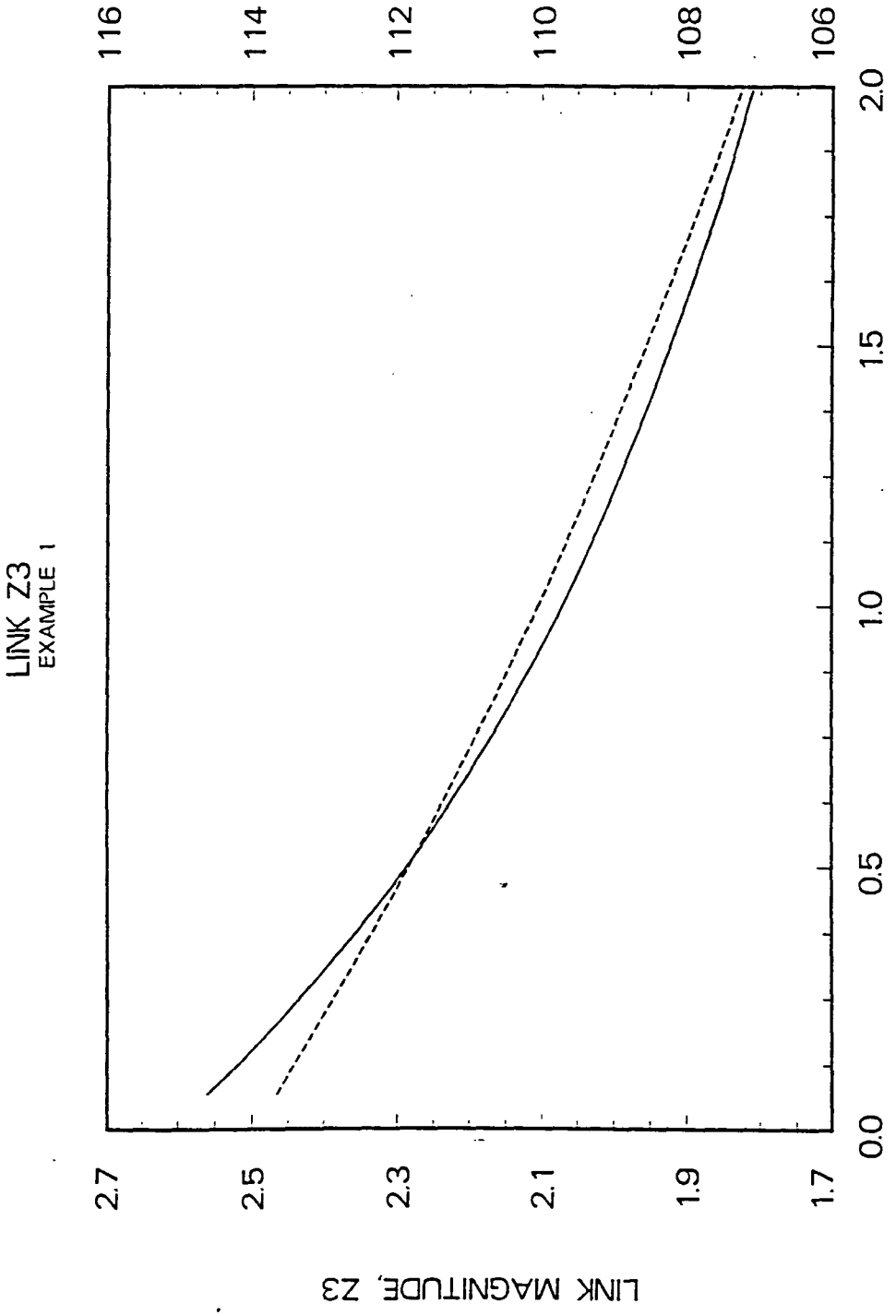

Figure 5.3 (Continued)

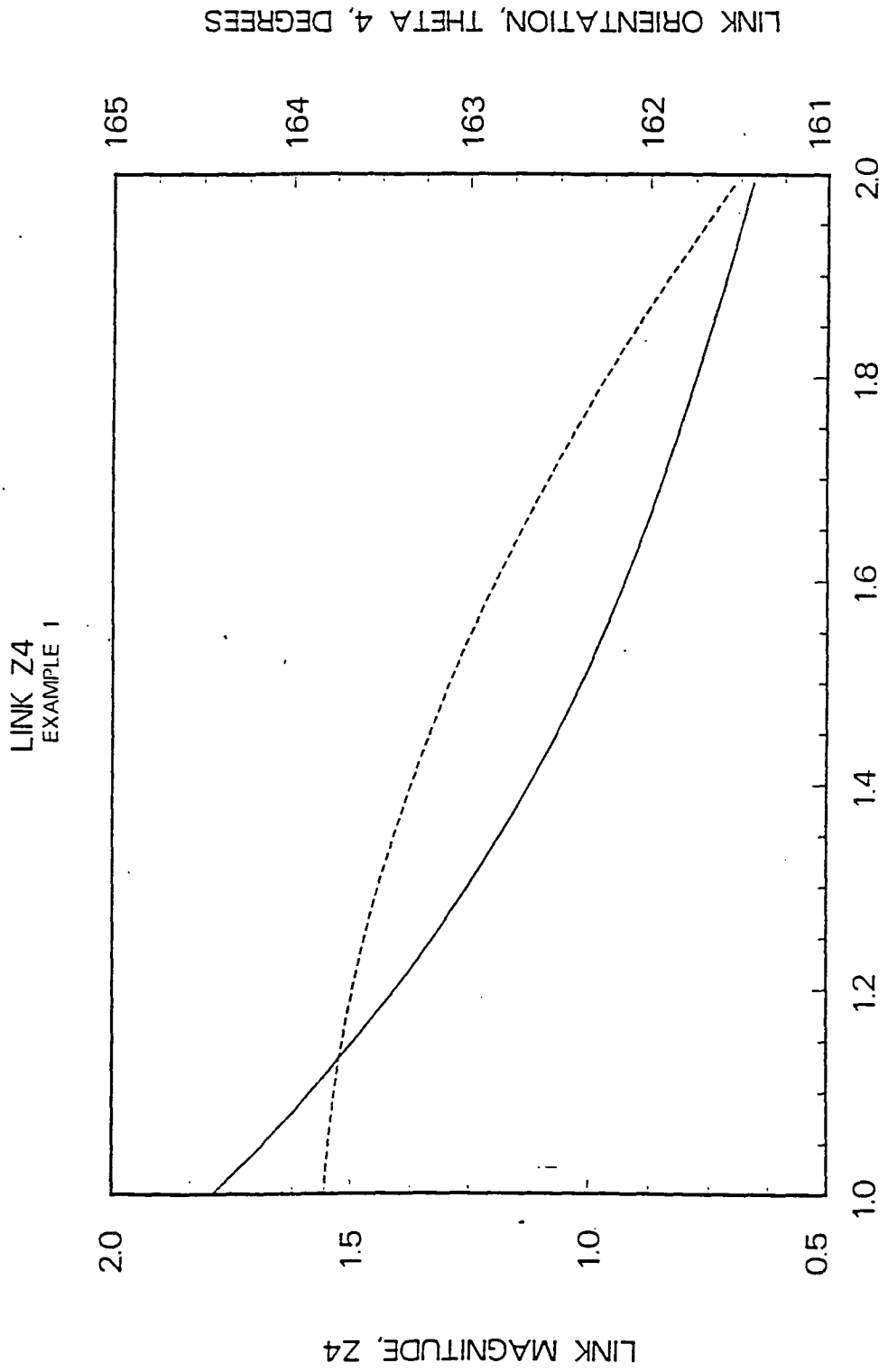

Figure 5.3 (Continued)

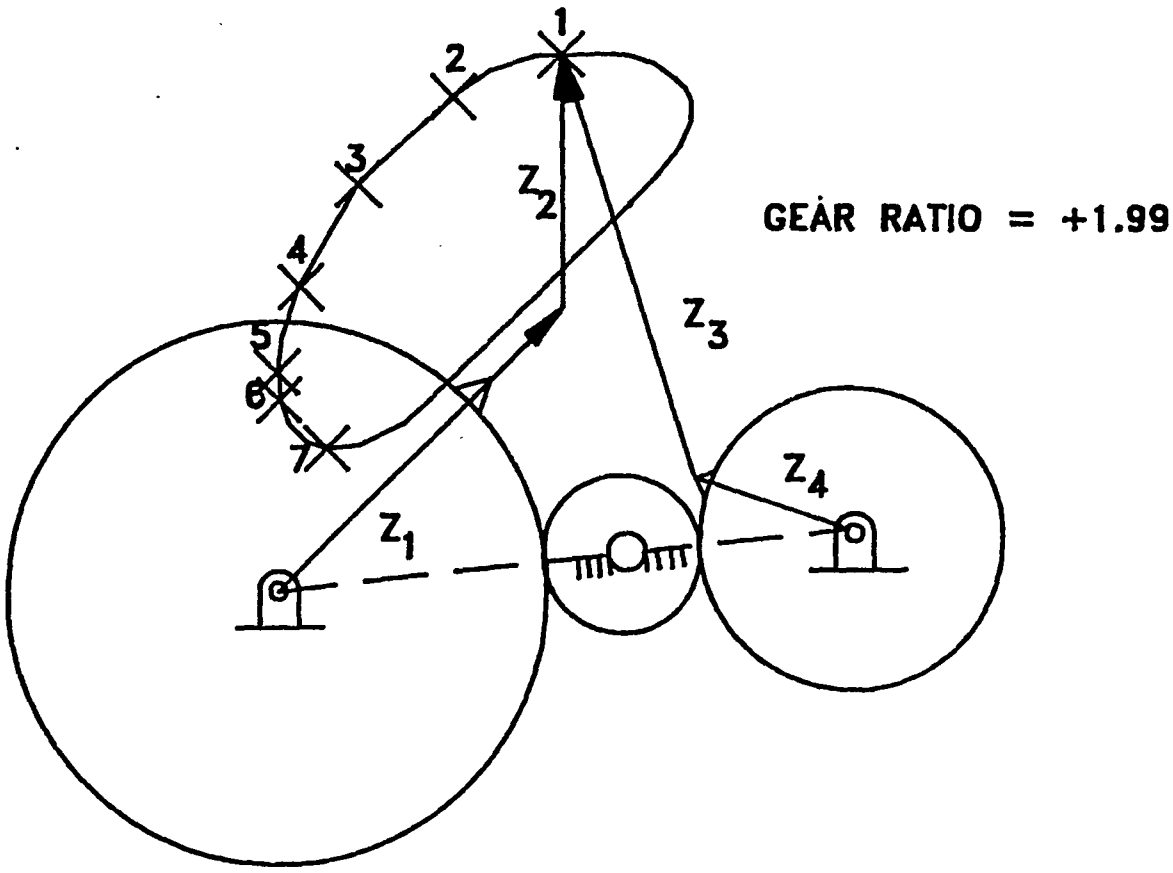

Figure 5.4: Five-bar mechanism and coupler path (Example 1)

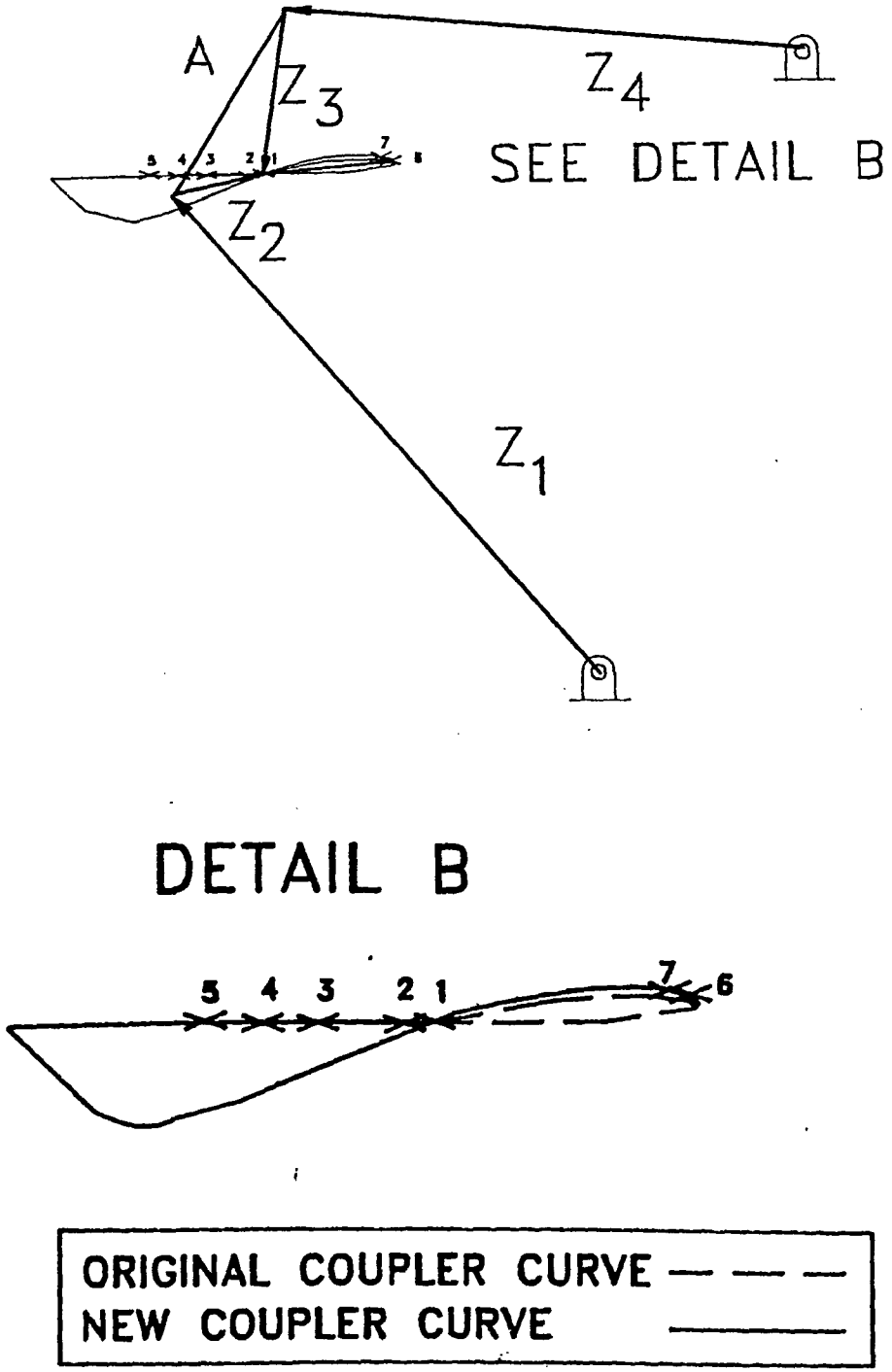

Figure 5.5: Original four-bar and coupler curve (Example 2)

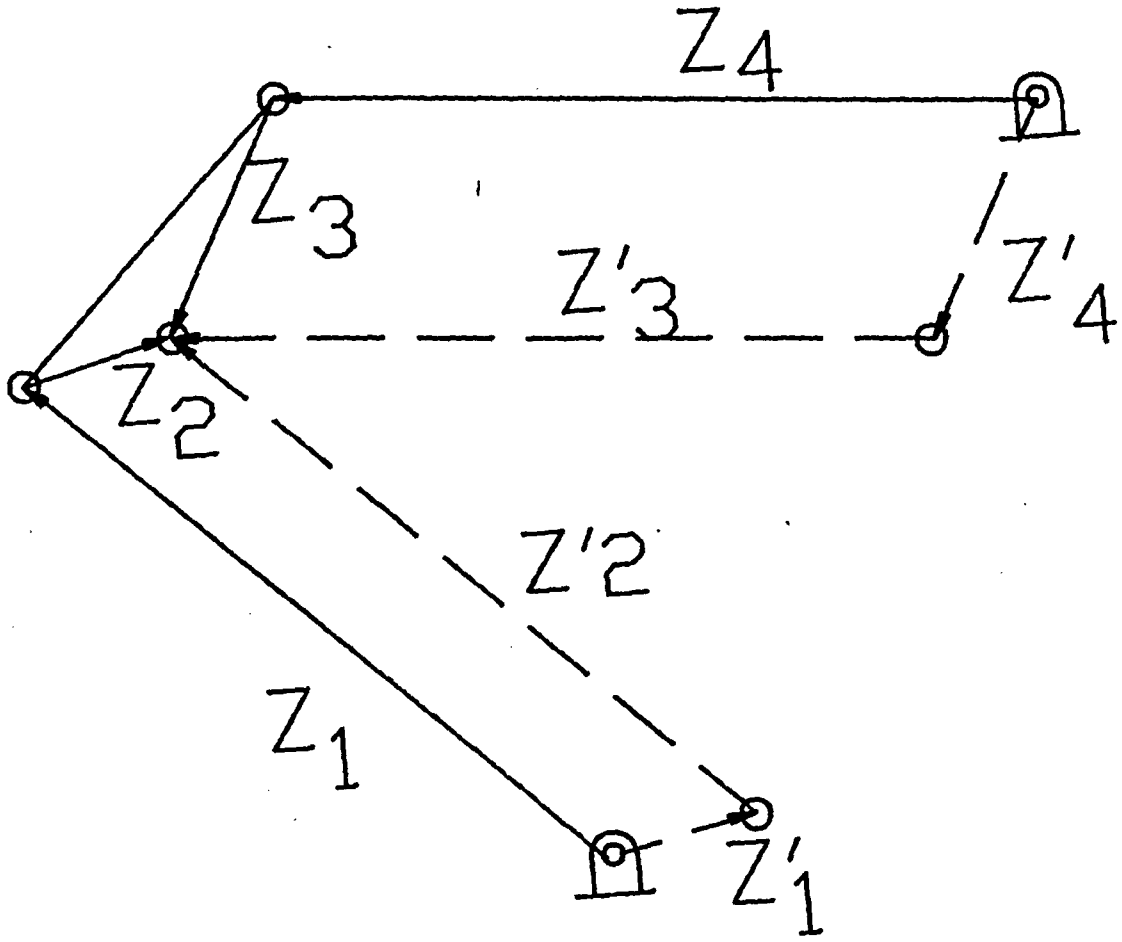

Figure 5.6: New four-bar and Robert's cognate (Example 2)

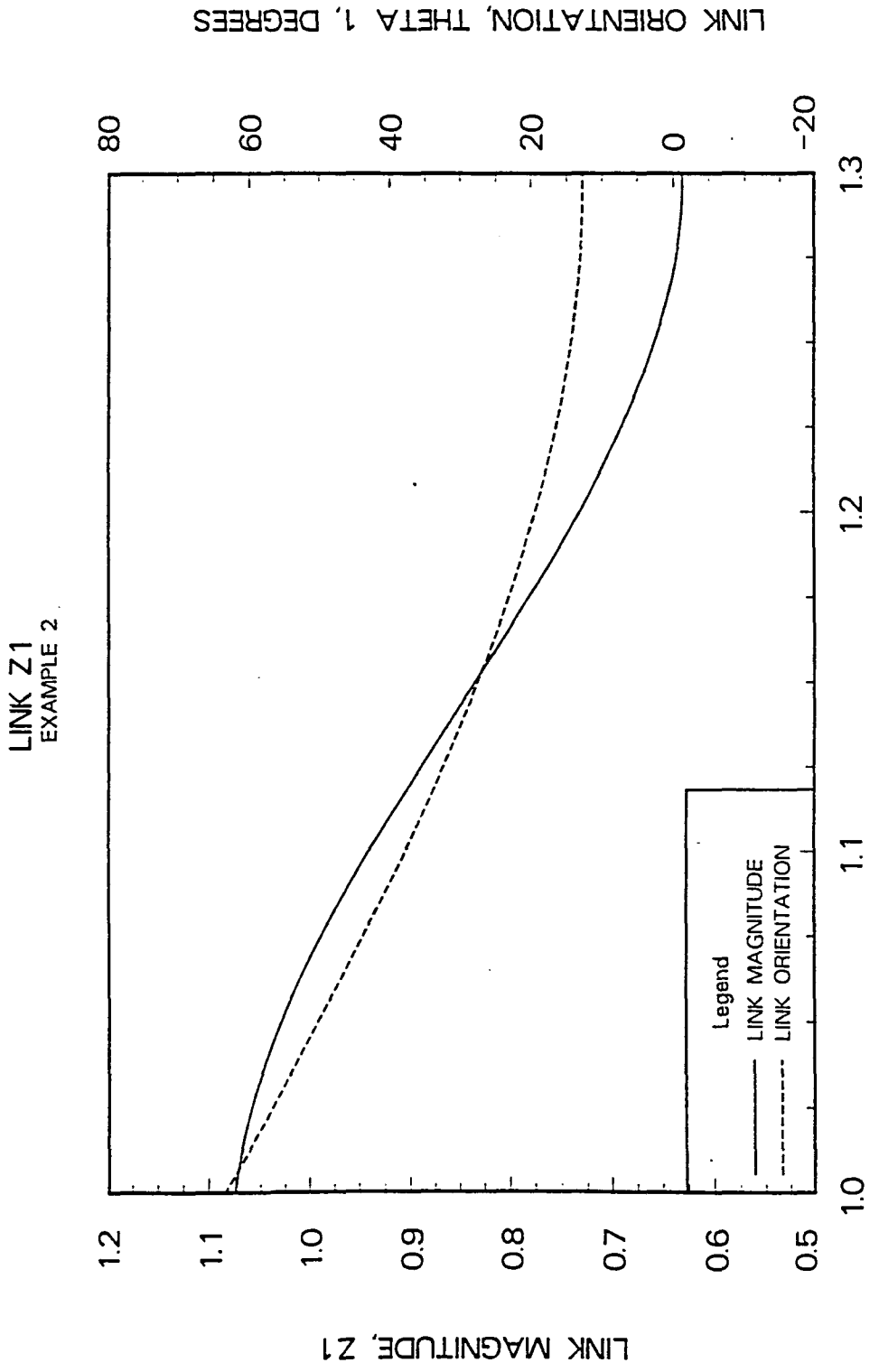

Figure 5.7: Link magnitudes and orientations with changing gear ratio (Example 2)

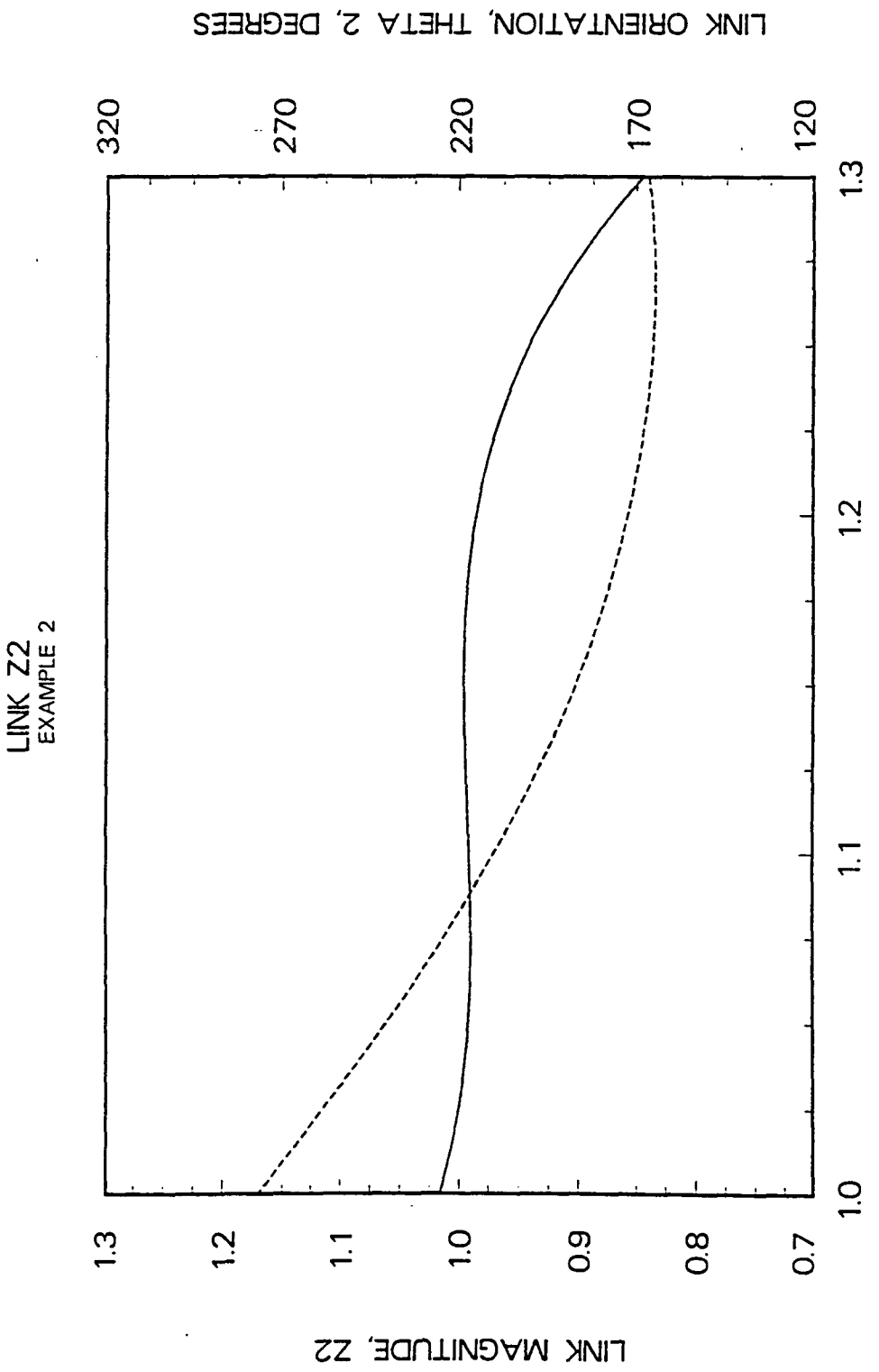

Figure 5.7 (Continued)

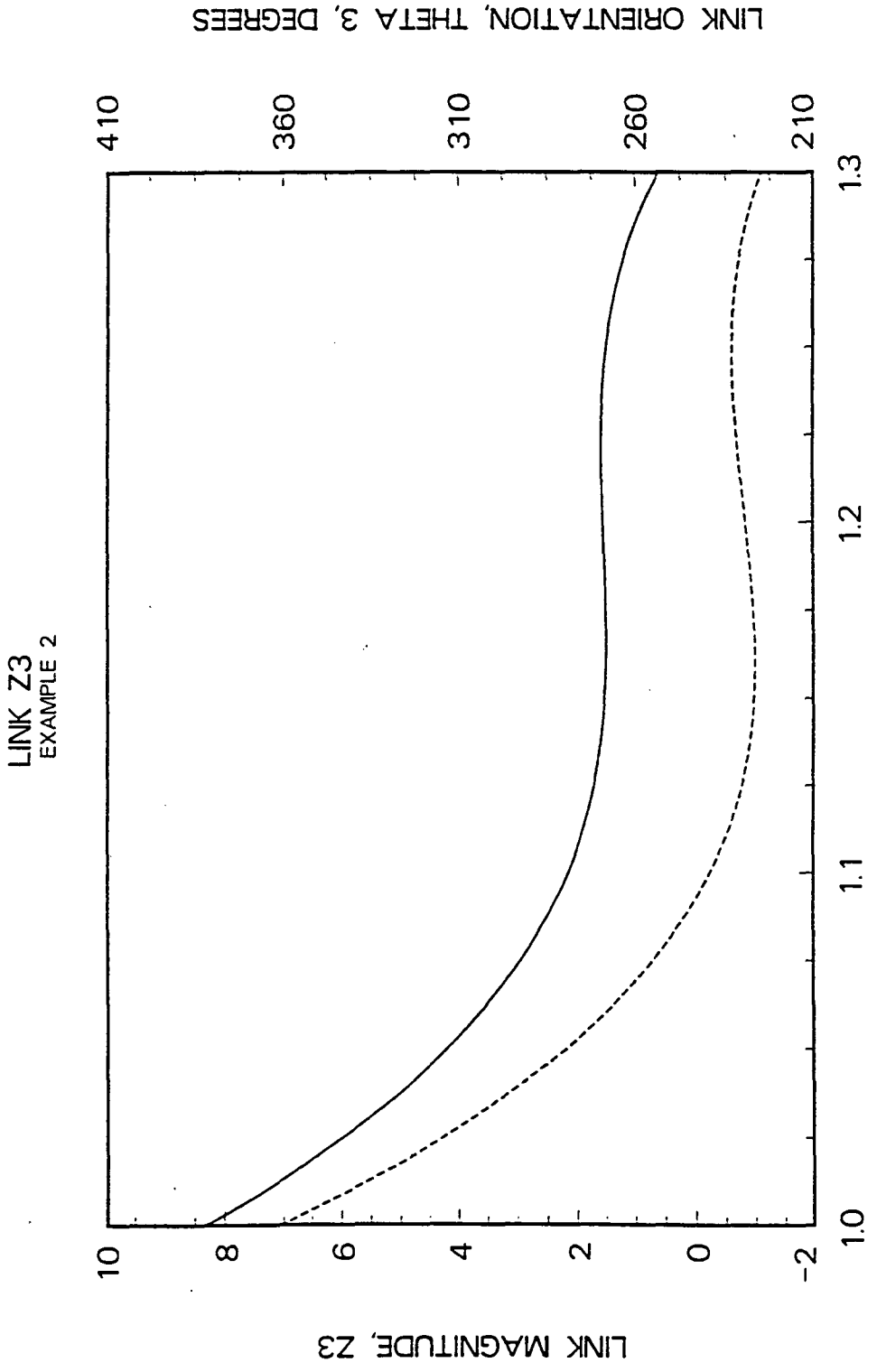

Figure 5.7 (Continued)

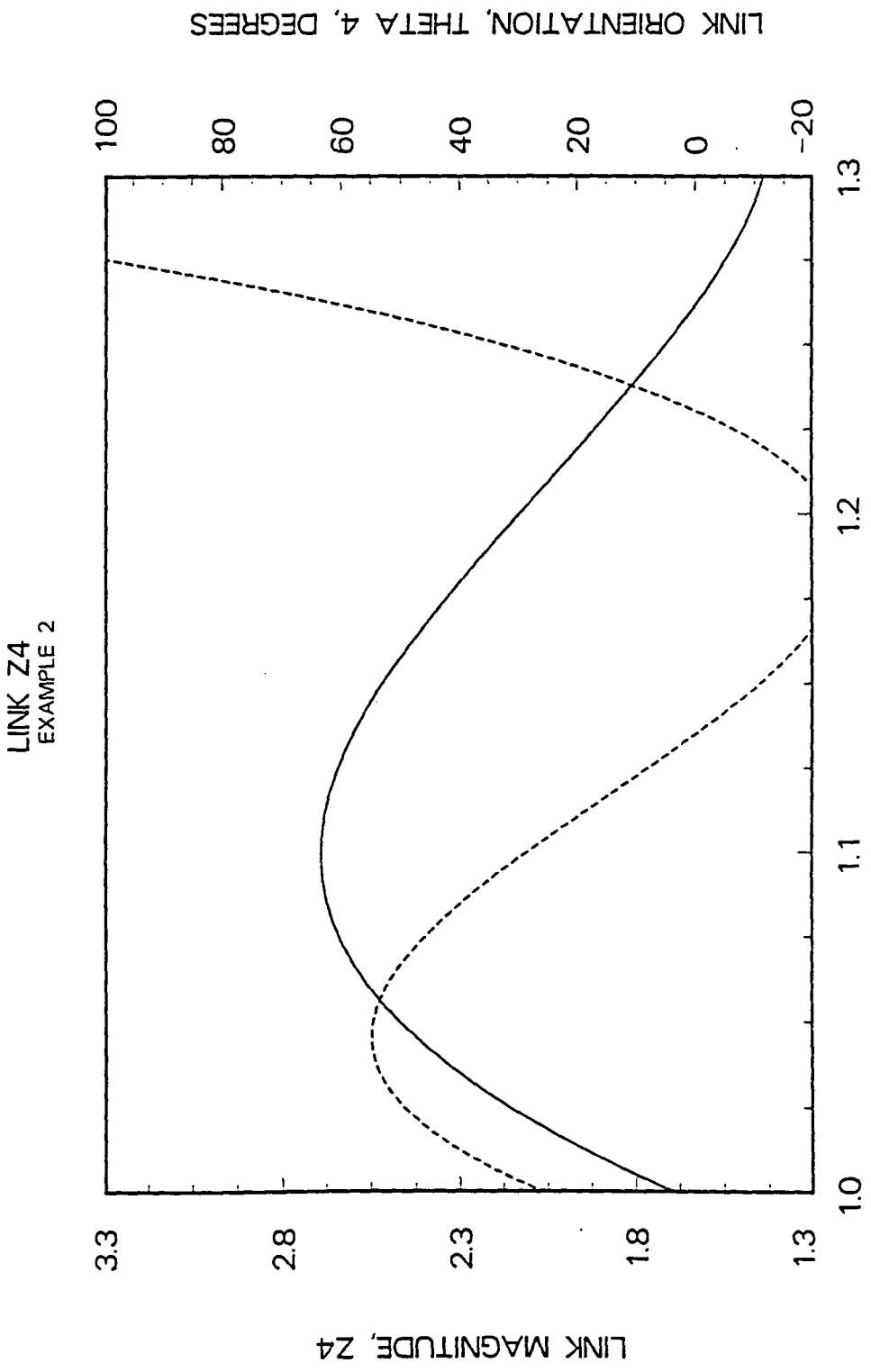

Figure 5.7 (Continued)

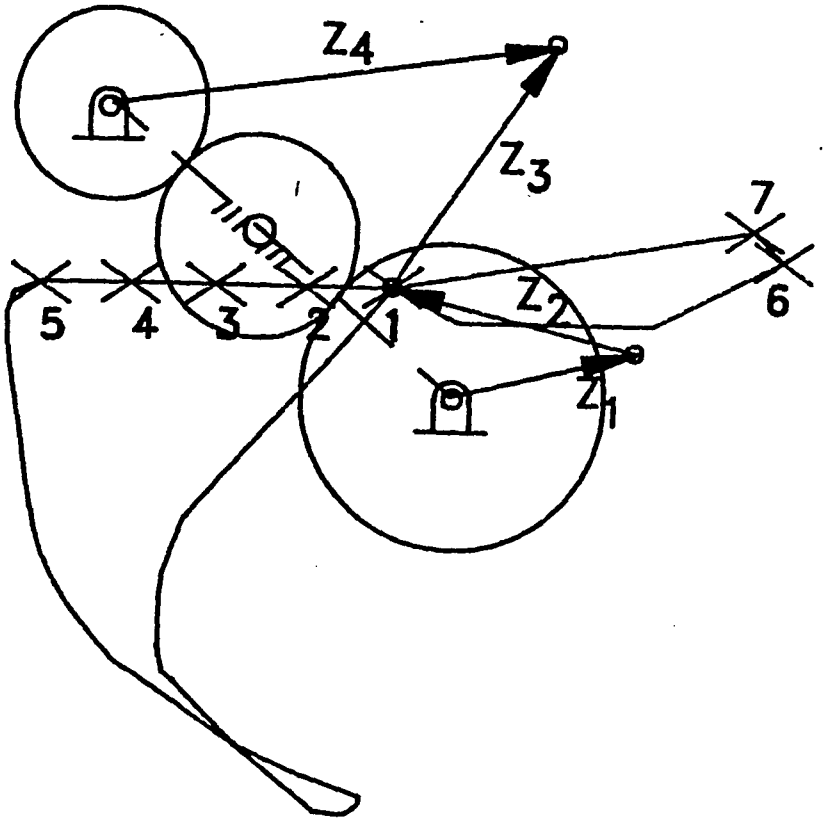

Figure 5.8: Five-bar mechanism and coupler path (Example 2)

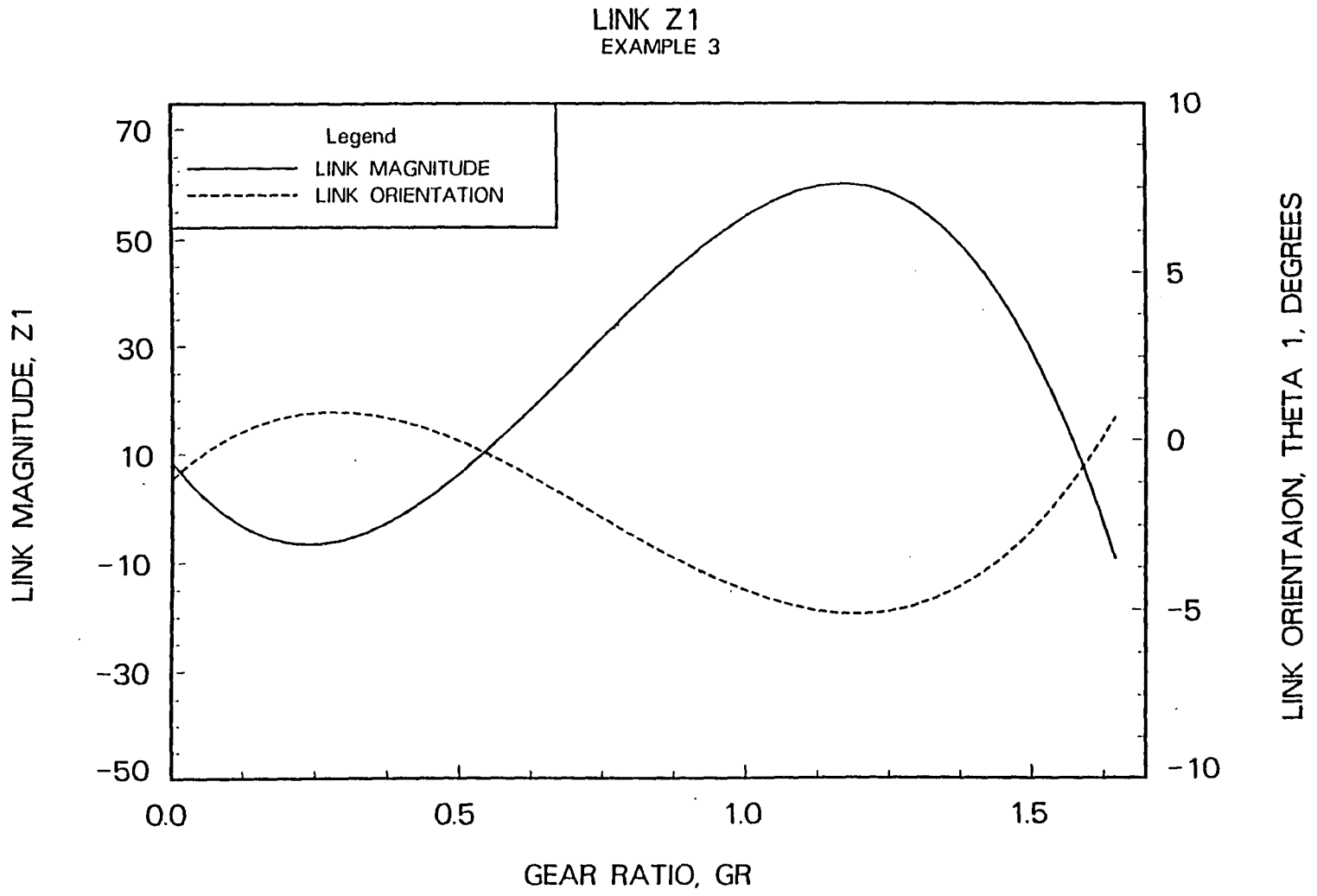

Figure 5.9: Changes in triad with gear ratio (Example 3)

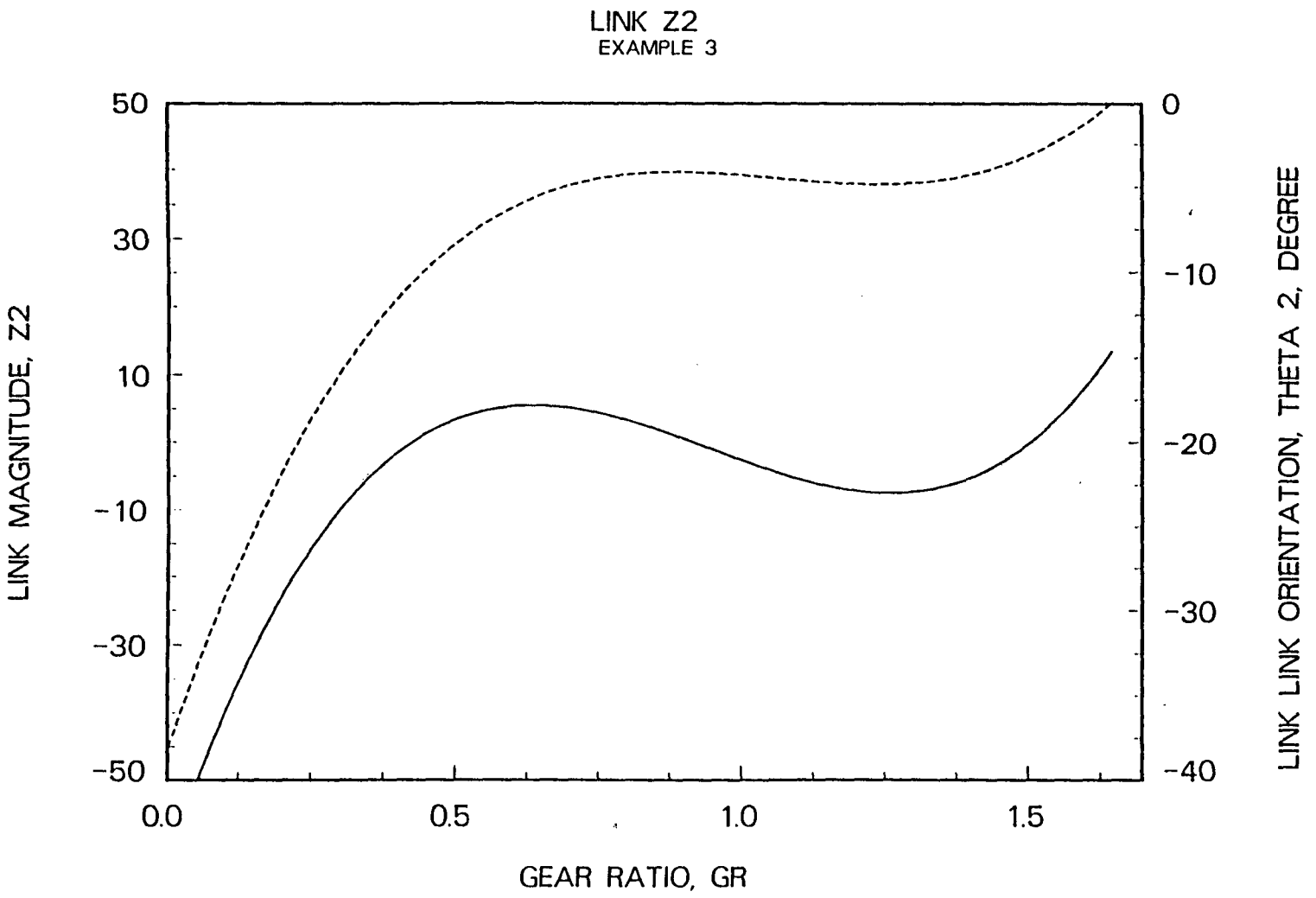

Figure 5.9 (Continued)

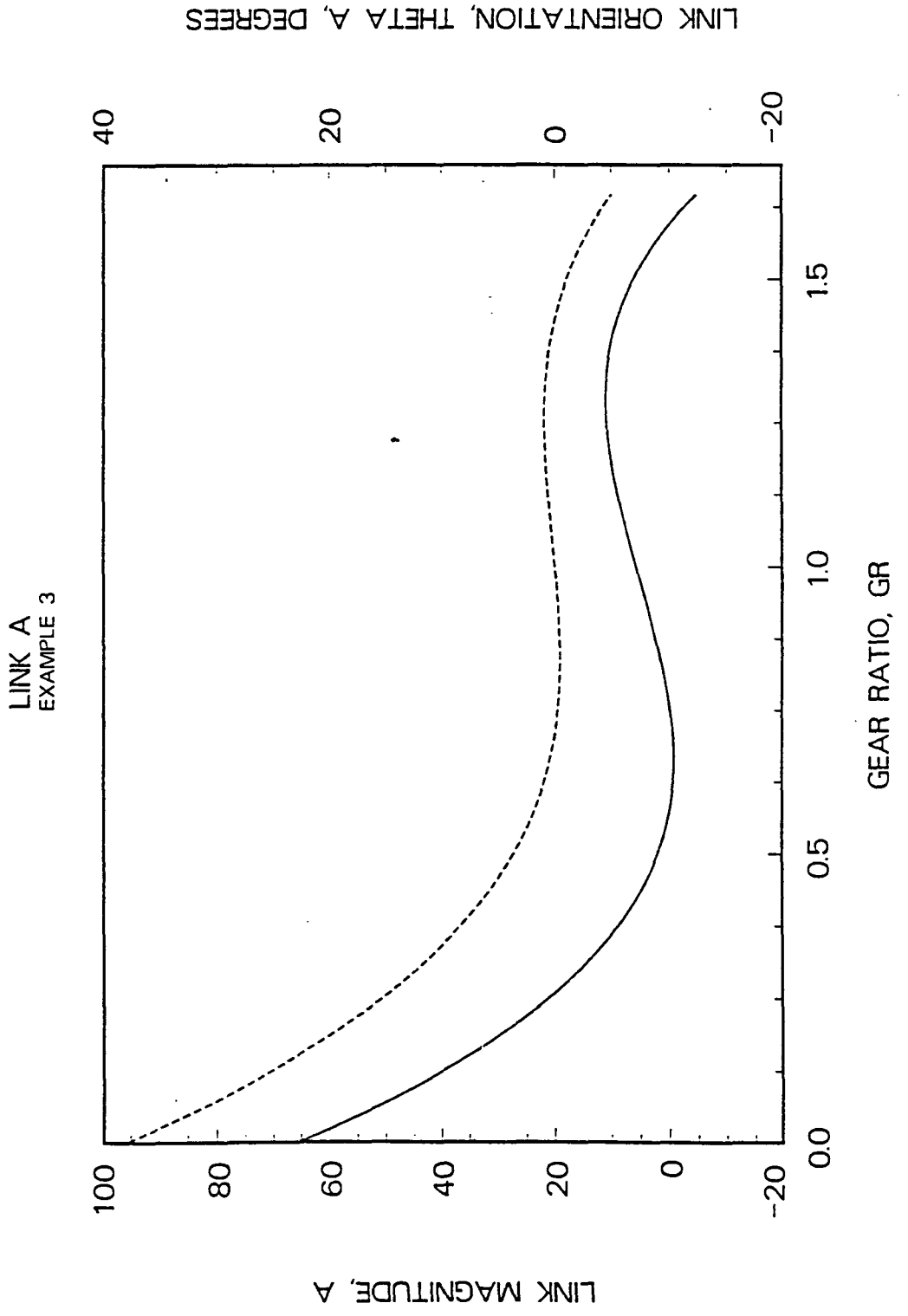

Figure 5.9 (Continued)

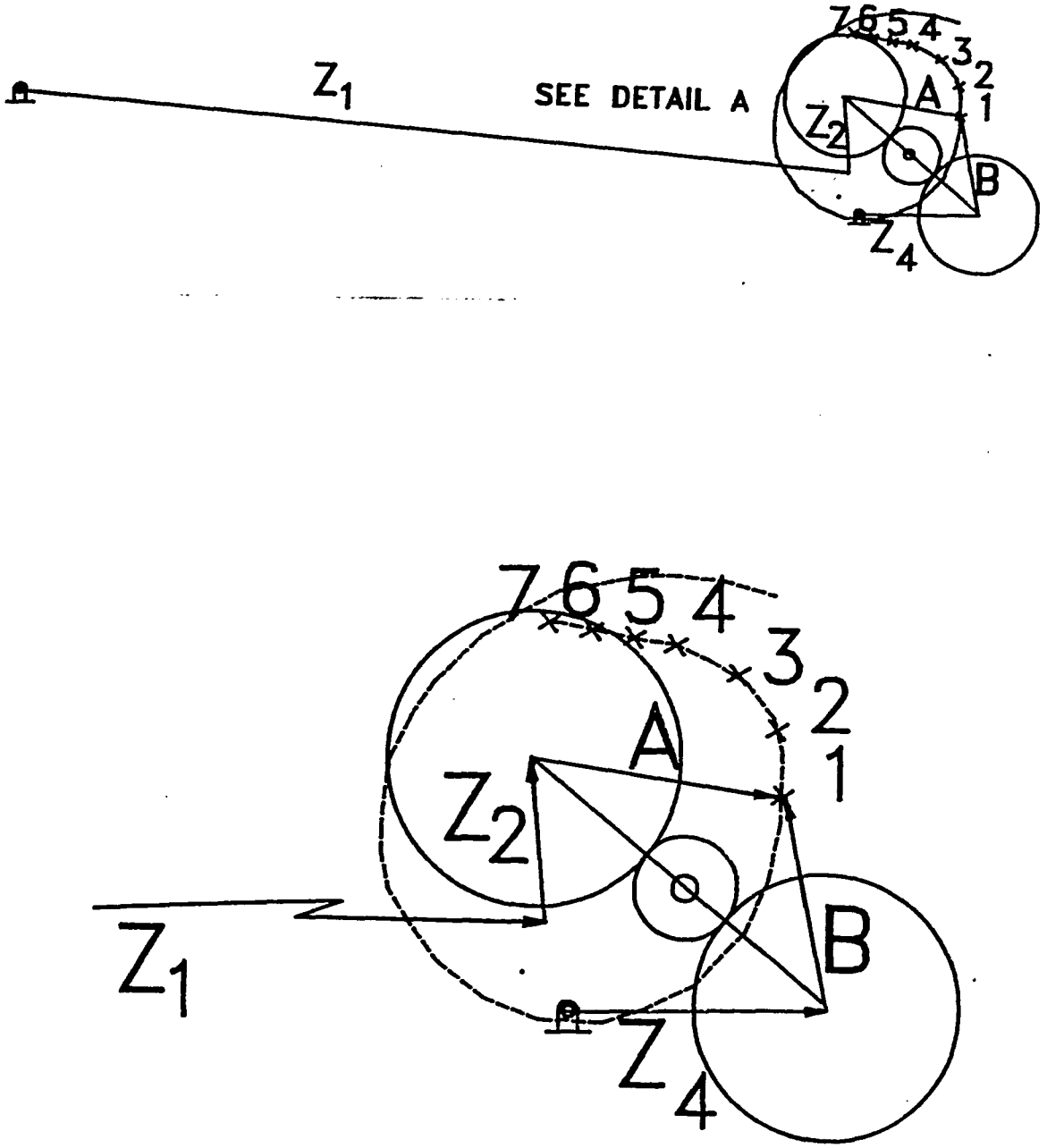

Figure 5.10: Coupler curve of triad-dyad five-bar (Example 3)

CHAPTER 6. RESULTS AND CONCLUSIONS

Continuation methods have been successfully implemented in the synthesis and design of four and five-bar linkages generating a prescribed path. Previous work demonstrated that five and nine point four-bar path generation could be accomplished through application of continuation methods (Subbian and Flugrad (1989), Tsai and Lu (1989), and Wampler, Morgan, and Sommese (1990)). Continued application of their work along with well posed numerical techniques has lead to the development of a method of synthesis culminating in a solution set of geared five-bar linkages. Subbian and Flugrad (1990) have also shown continuation methods to be useful in the design of considerably more complex mechansisms made up of triads and dyads. This work has lead to the subsequent development of an algorithm capable of examining a more complex gearing configuration.

Continuation methods provide numerous advantages not typically found in prevalent procedures. Traditional numerical methods of solution are heavily reliant on the "goodness" of initial values provided. Implied in this fact is that some knowledge of the system's behavior is known. Continuation methods alleviate the burden of providing "good" initial guesses.

Secondly, some continuation procedures find all solutions to system equations. Even though some of these solutions will be complex and others found at infinity,

not all solutions at infinity will be meaningless. Some solutions at infinity may be used to synthesize sliders in the case of four-bar mechanisms, and racks in the case of geared five-bar mechanisms. To find solutions, polynomial systems are required for continuation methods and kinematic synthesis in particular lends itself well to expression in polynomial form. Simple algebraic manipulation and various trigonometric identities have presently proven sufficient to provide equations amenable to continuation methods. Also solution sets of synthesis equations may be found using polynomial continuation. Conceding the fact that, in the case of the $N + 1$ method, the procedure may prematurely fail. However, whether or not the finally specified upper limit of integration is reached, the fact remains that a solution set has been found. In the case of the geared five-bar, seven precision point synthesis problem, the objective of finding linkage solutions over a range of gear ratios is still accomplished.

Finally, continuation methods have in the case of geared five-bars provided an avenue for exploring non-traditional synthesis problems. For example, variation of the gear ratio over a range of values and examination of more complex gearing configurations can be accomplished with continuation methods.

Disadvantages include the fact that continuation methods are CPU intensive. However, numerous techniques for easing CPU requirements, such as elimination of solutions at infinity, and homogenization of system equations are described and demonstrated by Morgan (1987).

Presently continuation methods are not in widespread use. However, continued research coupled with advancements in computer technology will provide an impetus for implementation of continuation methods for solution to numerous and diverse applications.

BIBLIOGRAPHY

Dhingra, A.K. and N.K. Mani. "Finite and Multiply Separated Kinematic Synthesis of Link and Geared Mechanisms." *Trends and Developments in Mechanics, Machines, and Robotics*, 1 (1988): 317–326.

Freudenstein, F. and B. Roth. "Synthesis of Path-Generating Mechansims by Numerical Methods." *Journal of Engineering for Industry*, 81B, No. 2 (1963): 298–306.

Li, T.Y., T. Sauer, and James Yorke. "Numerically Determining Solutions of Systems of Polynomial Equations." *Bulletin of the American Mathematical Society*, 18, No. 2 (April 1986): 173–177.

Morgan, Alexander. "A Method for Computing all Solutions to Systems of Polynomial Equations." *General Motors Publication-3651*, 1981.

Morgan, Alexander. *Solving Polynomial Systems Using Continuation for Engineering and Scientific Problems.* Englewood Cliffs, N.J.: Prentice-Hall, 1987.

Morgan, Alexander and Andrew Sommese. "Computing all Solutions to Polynomial Systems Using Homotopy Continuation." *Applied Mathematics and Computation*, 18 (1987): 115–138.

Morgan, A.P. and C.W. Wampler. "Sovling a Planar Four-Bar Design Problem Using Continuation." *Advances in Design Automation–1989: Mechanical Systems Analysis, Design and Simulation*, 19, No. 3 (1989): 409–416.

Sandor, G.N. and A.E. Erdman. *Advanced Mechanism Design: Analysis and Synthesis.* Englewood Cliffs, N.J.: Prentice-Hall, 1984.

Sandor, G.N., R.E. Kaufman, et al. "Kinematic Synthesis of Geared Linkages."

Journal of Mechanisms, 5, No. 1 (1969): 59–87.

Subbian, T. and D.R. Flugrad. "Four-Bar Path Generation Synthesis by a Continuation Method. *Advances in Design Automation-1989: Mechanical Systems Analysis, Design and Simulation* , 19, No. 3 (1989): 425–432.

Subbian, T. and D.R. Flugrad. "Six and Seven Position Triad Synthesis Using a Continuation Method." (Unpublished). Dept. of Mechanical Engineering, Iowa State University, Ames, IA, 1990.

Tsai, L.W. and J.J. Lu. "Coupler-Point-Curve Synthesis Using Homoptopy Methods." *Advances in Design Automation-1989: Mechanical Systems Analysis, Design and Simulation*, 19, No. 3 (1989): 417–424.

Wampler, C.W., A.P. Morgan and A.G. Sommese. "Numerical Continuation Methods for Solving Polynomial Systems in Kinematics." *General Motors Publication-6372*, 1982.

Wampler, C.W., A.P. Morgan and A.G. Sommese. "Complete Solution of the Nine-Point Synthesis Problem for Four-Bar Linkages." (Unpublished). Dept. of Mathematics, General Motors Research Laboratories, Warren, MI, 1990.

APPENDIX A. INVERSE KINEMATIC SOLUTION

The development given below details the derivation of angles ϕ_j and γ_j given the values of δ_{xj} and δ_{yj}, as well as the magnitude and initial position of vectors $\mathbf{Z_4}$ and $\mathbf{B}$. The angles Θ_B and Θ_4 are the orientations relative to the real axis of $\mathbf{Z_4}$ and $\mathbf{B}$, respectively. This method of closed form analysis is referred to throughout the preceding material as inverse kinematics. The loop closure equation for the dyad noted in Figure A.1 is:

$$\delta_j + \mathbf{Z_4}e^{i\Theta 4} + \mathbf{B}e^{i\Theta B} = \mathbf{Z_4}e^{i(\psi_j+\Theta_4)} + \mathbf{B}e^{i(\Theta_B+\gamma_j)} \tag{A.1}$$

Let:

$$\begin{aligned} \psi_j + \Theta_4 &= \rho_j \\ \gamma_j + \Theta_B &= \sigma_j \end{aligned} \tag{A.2}$$

The known parameter values are δ_{xj}, δ_{yj}, $\mathbf{Z_4}$, $\mathbf{B}$, Θ_4, and Θ_B. Separating real and imaginary components:

$$\begin{aligned} &REAL: \\ &\quad R_x = \delta_{xj} + Z_4 cos\Theta_4 + B cos\Theta_B \\ &IMAGINARY: \\ &\quad R_y = \delta_{yj} + Z_4 sin\Theta_4 + B sin\Theta_B \end{aligned} \tag{A.3}$$

The magnitude of R is given by:

$$R = \sqrt{R_x^2 + R_y^2} \tag{A.4}$$

The orientation of vector **R** is given by:

$$\Theta_R = ATAN2(R_y, R_x) \tag{A.5}$$

where "ATAN2" is an intrinsic FORTRAN function that finds the tangent of an angle in its correct quadrant. Rewriting Eq. (A.1) in terms of R we have:

$$Re^{i\Theta}R = Z_4 e^{i\rho_j} + Be^{i\sigma_j} \tag{A.6}$$

Moving $Z_4 e^{i\rho_j}$ to the left hand side of Eq. (A.6) results in,

$$Re^{i\Theta}R - Z_4 e^{i\rho_j} = Be^{i\sigma} \tag{A.7}$$

Now, dividing Eq. (A.7) into real and imaginary parts gives,

$$\begin{aligned} Rcos\Theta_R - Z_4 cos\rho_j &= Bcos\sigma_j \\ Rsin\Theta_R - Z_4 sin\rho_j &= Bsin\sigma_j \end{aligned} \tag{A.8}$$

Squaring the results of this equation and adding them gives,

$$R^2 + Z_4^2 - 2RZ_4 cos(\Theta_R - \rho_j) = B^2 \tag{A.9}$$

Parameters ρ_j and then ψ_j are found as follows:

$$\begin{aligned} \rho_j &= \Theta_R \pm ACOS(\frac{Z_4^2 + R^2 - B^2}{2RZ_4}) \\ \psi_j &= \rho_j - \Theta_4 \end{aligned} \tag{A.10}$$

Now that the values of ρ_j and ψ_j are known, σ_j may be found.

$$\begin{aligned} Rcos\Theta_R - Z_4 cos\rho_j &= Bcos\sigma_j \\ Rsin\Theta_R - Z_4 sin\rho_j &= Bsin\sigma_j \end{aligned} \tag{A.11}$$

The value of σ_j results by finding the tangent of $\frac{Bsin\sigma_j}{Bcos\sigma_j}$. Finally, the angular displacement of link B, γ_j is realized with,

$$\gamma_j = \sigma_j - \Theta_B \tag{A.12}$$

The reader should note that two possible orientations for each angular displacment are possible. This fact manifests itself when the mechanism of question "branches" to form a "mirror" image.

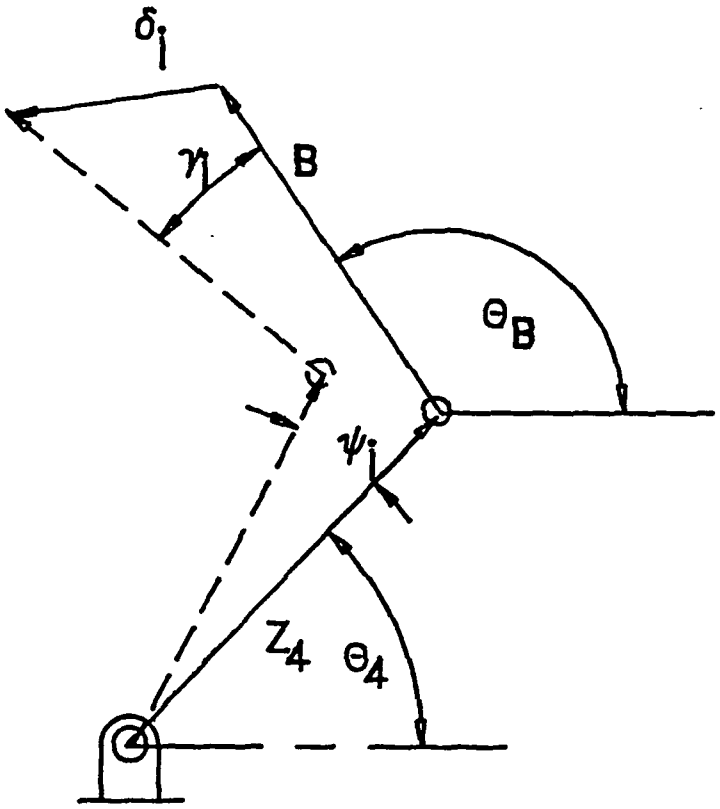

Figure A.1: Dyad for kinematic analysis shown in the jth position

APPENDIX B. KINEMATIC ANALYSIS

The following developments were utilized to generate numerical values and subsequently, graphical depiction of the coupler curve's created by the mechanisms synthesized in this paper.

For the four-bar mechanism depicted in Figure B.1 the development that follows describes the position of point P for any value of Θ_1. The known parameters in this procedure are $\mathbf{Z_1}$, $\mathbf{Z_2}$, $\mathbf{Z_3}$, $\mathbf{Z_4}$, $\mathbf{Z_5}$, A, and Θ_1. Also known are angles ϵ, β and λ, the angles comprising the geometry of the coupler link. The value of the reference vector, l, and its orientation relative to the real axis, may be found as follows:

$$\mathbf{Z_1}e^{i\Theta}1 = \mathbf{Z_5}e^{i\Theta}5 + \mathrm{l}e^{i\eta} \tag{B.1}$$

The x and y components of l are:

$$\begin{aligned} l_x &= Z_1 cos\Theta_1 - Z_5 cos\Theta_5 \\ l_y &= Z_1 sin\Theta_1 - Z_5 sin\Theta_5 \\ l &= \sqrt{l_x^2 + l_y^2} \end{aligned} \tag{B.2}$$

The orientation of l in the j^{th} (η_j) position may be found by finding the tangent of $\frac{l_y}{l_x}$.

Writing an equation around loop $\mathrm{l} - \mathbf{Z_4} - \mathrm{A}$ gives:

$$\mathbf{Z_4}e^{i\Theta}4 + \mathrm{A}e^{i\Theta}A = \mathrm{l}\mathbf{e}^{\mathrm{i}\eta\mathrm{j}} \tag{B.3}$$

Movement of $\mathbf{Ae^{i\Theta A}}$ to the right hand side and separation into real and imaginary parts, followed by squaring and addition of the resulting equations gives an expression that may be use to solve for Θ_A.

$$\Theta_A = \eta_j \pm ACOS(\frac{A_2 + l^2 - Z_4^2}{2lA}) \tag{B.4}$$

Now Θ_3 may be found noting that $\Theta_3 = \Theta_A - \epsilon$.

The position of point P, relative to the ground pivot of link $\mathbf{Z_1}$ is:

$$\mathbf{R_p} = \mathbf{Z_1}e^{i\Theta}1 - \mathbf{A}e^{i\Theta}A + \mathbf{Z_3}e^{i\Theta}3 \tag{B.5}$$

Dividing this expression in real and imaginary parts yields,

$$\begin{aligned} R_x &= Z_1 cos\Theta_1 - Acos\Theta_A + Z_3 cos\Theta_3 \\ R_y &= Z_1 sin\Theta_1 - Asin\Theta_A + Z_3 sin\Theta_3 \end{aligned} \tag{B.6}$$

The values of R_x and R_y may also be expressed relative to the initial position of the coupler point P, hence the first precision point will always have coordinates (0.0,0.0).

The analysis procedure for a geared five-bar like that shown in Figure B.2 is simplified by the fact that the gearing relationship provides an additional known parameter. Recalling that the displacement of link $\mathbf{Z_1}$, ϕ_j, is related to the displacement of link $\mathbf{Z_4}$ through the equation $\psi_j = GR * \phi_j$, it can be seen that by stepping values of Θ_1 in increments of ϕ_j, Θ_4, for any Θ_1 may be computed from:

$$\Theta_4 = \Theta_{4i} + \psi_j \tag{B.7}$$

where Θ_{4i} is the initial value of Θ_4.

Now the magnitude and direction of reference vector l may be found by writing the loop closure equation around loop $\mathbf{l - Z_5 - Z_4}$.

$$\mathbf{l}e^{i\nu_j} = \mathbf{Z_5}e^{i\Theta}5 + \mathbf{Z_4}e^{i\Theta}4$$

$$
\begin{aligned}
l_x &= Z_5 cos\Theta_5 + Z_4 cos\Theta_4 \\
l_y &= Z_5 sin\Theta_5 + Z_4 sin\Theta_4 \\
l &= \sqrt{l_x^2 + l_y^2} \\
\nu_j &= tan^{-1}\frac{l_y}{l_x}
\end{aligned}
\tag{B.8}
$$

The loop comprising the vectors $\mathbf{Z_1 - l - A}$ gives,

$$
\mathbf{Z_1} e^{i\Theta 1} = \mathbf{l} e^{i\nu_j} + \mathbf{A} e^{i\Theta a} \tag{B.9}
$$

Rearrangement of Eq.(B.9) such that $Ae^{i\Theta}A$ is on the left hand side, followed by solution for the x and y components of **A** gives,

$$
\begin{aligned}
A_x &= Z_1 cos\Theta_1 - l cos\nu_j \\
A_y &= Z_1 sin\Theta_1 - l sin\nu_j
\end{aligned}
\tag{B.10}
$$

The magnitude and direction of **A** are found as follows:

$$
\begin{aligned}
A &= \sqrt{A_x^2 + A_y^2} \\
\Theta_A &= tan^{-1}\frac{A_y}{A_x}
\end{aligned}
\tag{B.11}
$$

The parameter,Θ_2 ,may be found by writing the loop closure equation for loop $A - Z_2 - Z_3$.

$$
\mathbf{Z_3} = \mathbf{A} e^{i\Theta}A + \mathbf{Z_2} e^{i\Theta 2} \tag{B.12}
$$

Squaring this equation gives:

$$
Z_3^2 = A^2 + Z_2^2 + 2AZ_2 cos(\Theta_2 - \Theta_A) \tag{B.13}
$$

The parameter Θ_2 is found by,

$$\Theta_2 = \Theta_A \pm ACOS\left[\frac{-Z_3^2 + A^2 + Z_2^2}{2AZ_2}\right] \tag{B.14}$$

Now the position of the coupler point, relative to the ground pivot of link Z_1, for any Θ_1 may be described by:

$$\mathbf{R_p} = \mathbf{Z_1}e^{i\Theta 1} + \mathbf{Z_2}e^{i\Theta 2} \tag{B.15}$$

The x and y components of the coupler point, relative to the ground pivot of link Z_1 would be:

$$\begin{aligned} R_{px} &= Z_1 cos\Theta_1 + Z_2 cos\Theta_2 \\ R_{py} &= Z_1 sin\Theta_1 + Z_2 sin\Theta_2 \end{aligned} \tag{B.16}$$

Also, the location of the coupler point may be expressed relative to its initial position, in which case the first precision coordinates would be (0.0,0.0) and subsequent points would be calculated by determining $\mathbf{R_p}$ at the "current" value of Θ_1 and subtracting the value of $\mathbf{R_p}$ at the very first position.

The final analysis procedure finds the position of the coupler point for the five-bar mechanism shown in Figure 4.1. The known parameters are $\mathbf{Z_1}$, $\mathbf{Z_2}$, **A**,**B**, $\mathbf{Z_4}$, and $\mathbf{Z_5}$. Also the initial values of the orientations of each link are known and are designated by the subscript i. So, for instance, $\Theta_1 = \Theta_{1i} + \phi_j$, where j is the value of ϕ at the j^{th} position of the mechanism. It must be noted that at every position of the linkage, the gearing relationship must be enforced. Writing a closure equation around loop $\mathbf{Z_1 - Z_2 - A - B - Z_4}$ gives:

$$\mathbf{Z_1}e^{i(\Theta_{1i}+\phi_j)} + \mathbf{Z_2}e^{i(\Theta_{2i}+\alpha_j)} + \mathbf{A}e^{i(\Theta_{A_i}+\gamma_j)} = \mathbf{Z_5}e^{i\Theta_5} + \mathbf{Z_4}e^{i(\Theta_{4i}+\psi_j)} + \mathbf{B}e^{i\Theta_B} \tag{B.17}$$

The gearing relationship is given by,

$$\alpha_j = \gamma_j + \left[\gamma_j - \psi_j\right] GR \tag{B.18}$$

Equation (B.18) may be divided into real and imaginary components, with each component equation arranged such that the right hand side is equal to 0.0.

$$\begin{aligned} 0 &= Z_1 cos(\Theta_{1i} + \phi_j) + Z_2 cos(\Theta_{2i} + \alpha_j) + A cos(\Theta_{Ai} + \gamma_j) \\ &- Z_5 cos\Theta_5 - B cos(\Theta_{Bi} + \gamma_j) - Z_4 cos(\Theta_{4i} + \psi_j) \\ 0 &= Z_1 sin(\Theta_{1i} + \phi_j) + Z_2 sin(\Theta_{2i} + \alpha_j) + A sin(\Theta_{Ai} + \gamma_j) \\ &- Z_5 sin\Theta_5 - B sin(\Theta_{Bi} + \gamma_j) - Z_4 sin(\Theta_{4i} + \psi_j) \end{aligned} \tag{B.19}$$

Enforcement of the gearing relationship must also include a measure to ensure that trigonometric realtionships are preserved. The trigonometric identity that follows was used as the third of three residual functions to be solved:

$$sin^2(\gamma_j + GR * (\gamma_j - \psi_j)) + cos^2(\gamma_j + GR * (\gamma_j - \psi_j)) = 1 \tag{B.20}$$

Since Eqs.(B.18), (B.19), and (B.20) must be solved simultaneously, an iterative technique is necessary to find the unknown parameters ϕ_j, ψ_j, and γ_j. The displacement of link **A**, α_j, is the incremental change in angle Θ_A and is stepped until the rotation of **A** has reached 360^o.

The equation solver implemented for simultaneous solution of Eqs.(B.19) and (B.20) was Newton-Raphson.

Once the values of the unknown angular displacments have been determined, the position of the coupler point may be determined from:

$$\mathbf{R_p} = \mathbf{Z_1} e^{i(\Theta_{1i} + \phi_j)} + \mathbf{Z_2} e^{i(\Theta_{2i} + \alpha_j)} \tag{B.21}$$

The x and y coordinates of the coupler point, P, may be expressed relative to the ground pivot of link $\mathbf{Z_1}$, or as previously shown, subsequent values of R_p may be subtracted from the initial value of R_p to yield coordinates relative to the first position on the coupler path.

$$\begin{aligned} \delta_{xj} &= R_{px} - R_{pxi} \\ \delta_{yj} &= R_{py} - R_{pyi} \end{aligned} \tag{B.22}$$

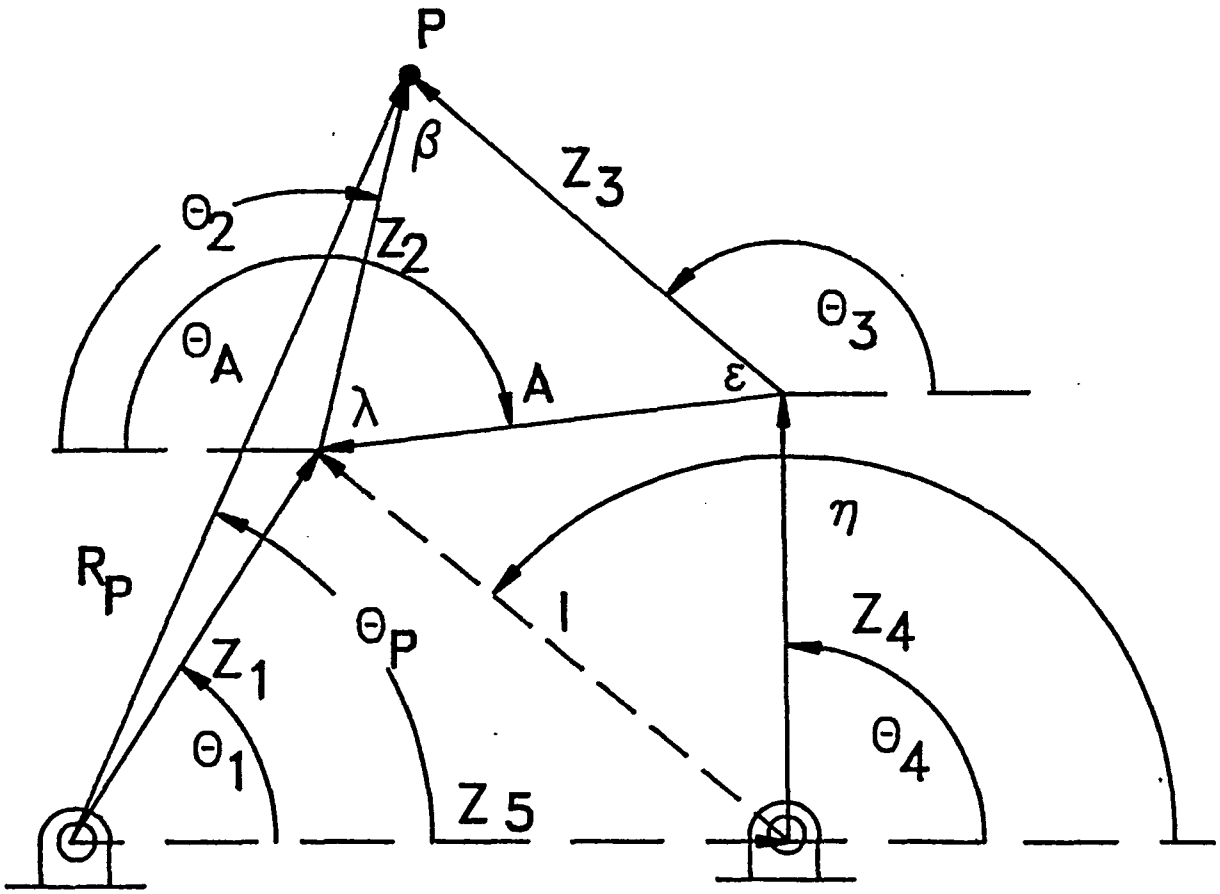

Figure B.1: Planar four-bar mechanism in the jth postion

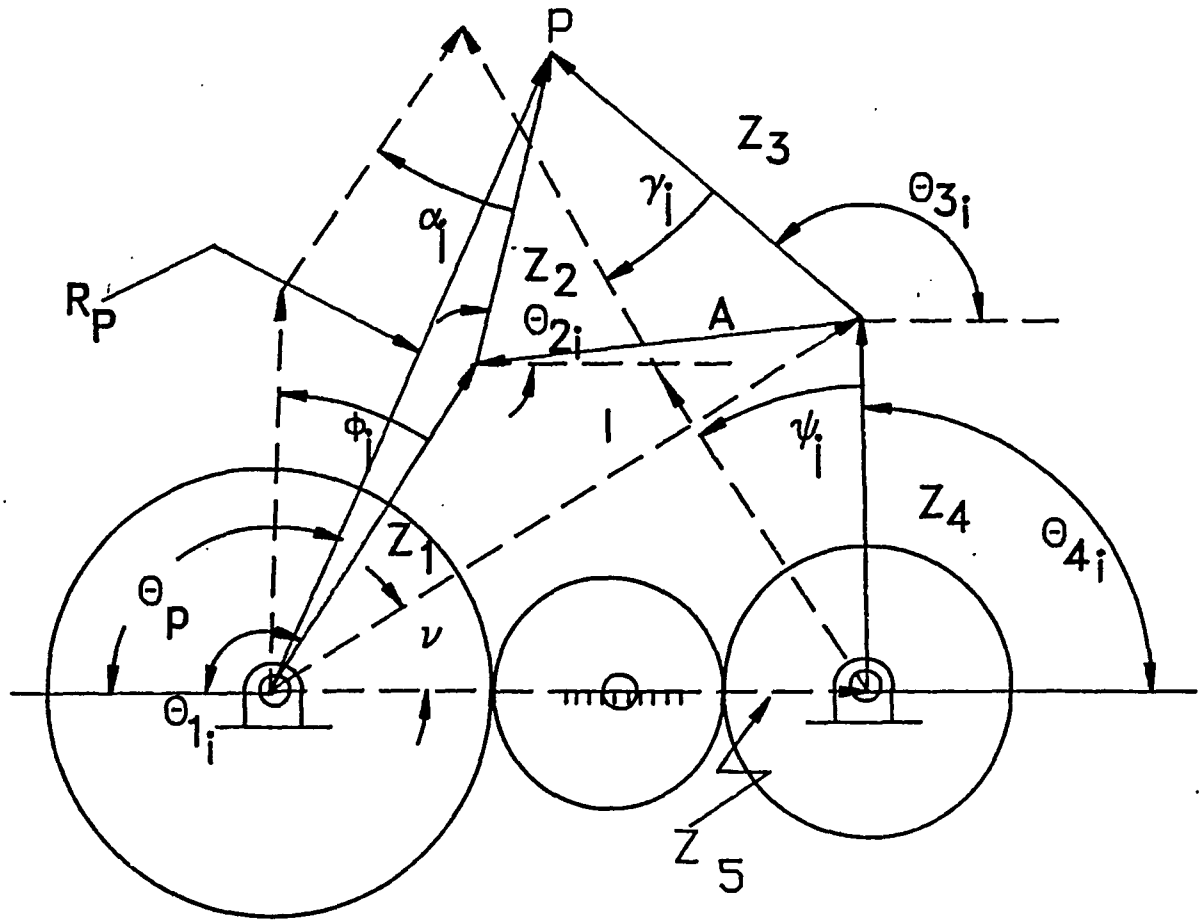

Figure B.2: Planar geared five-bar mechanism